3B Containment Hydrodynamic Loads

3B.1 Introduction

3B.1.1 Purpose

This appendix provides a description and load definition methodology for hydro-dynamic loading conditions inside the primary containment in an Advanced Boiling Water Reactor (ABWR) during safety/relief valve (SRV) actuation and a loss-of-coolant accident (LOCA) events. Overall, the load definition methodology used for the ABWR containment design is similar to that used for prior BWR containment designs. Wherever the ABWR unique design features warranted additional information for defining ABWR design loads, ABWR unique analyses and tests were conducted to provide an adequate database for defining the pertinent hydrodynamic loads.

3B.1.2 ABWR Containment Design Features

Subsection 6.2.1.1.2 provides a description of the design features of the ABWR containment system. The basic ABWR containment features are shown in Figure 3B-1. The ABWR design utilizes a horizontal vent system that is similar to the prior Mark III design, but includes some design features which are unique to the ABWR. These unique features include pressurization of the wetwell gas space, the presence of a lower drywell (L/D), the smaller number of horizontal vents (30 in ABWR vs. 120 in Mark III), extension of horizontal vents into the pool, vent submergence, and suppression pool width.

3B.2 Review of Phenomena

This section describes the sequence of events occurring during safety/relief valve (SRV) actuations and a postulated LOCA, and describes the potential load producing conditions. A spectrum of break sizes is considered for the LOCA event.

3B.2.1 Safety/Relief Valve Actuation

SRVs are utilized in a BWR pressure suppression system to provide pressure relief during certain reactor transients. Steam discharge through the SRVs is routed through discharge lines into the pressure suppression pool, where it is condensed. Each discharge pipe is fitted at the end with a device called a quencher to promote heat transfer during SRV actuation between the high temperature compressed air and steam mixture and the cooler water in the suppression pool. This enhances heat transfer results in a low amplitude oscillating pressure in the pool and eliminates concern over operation at high suppression pool temperature. For ABWR plants, the discharge device is an X-quencher which has been used for prior plants.

SRV actuation may occur (1) in response to a reactor system transient pressure increase (pressure actuation), (2) as the result of planned operator action (manual operation), or (3) as the result of a failure or error affecting one SRV (inadvertant opening). Inadvertant operation involves a single SRV, as does manual operation. Pressure actuation involves from one to all

SRVs opening sequentially during the vessel pressure rise. The opening sequence depends on the SRV pressure setpoints.

The discharge piping of an SRV contains ambient air and a column of water whose volume determined by (1) the submergence and inclination of the SRV discharge line in the suppression pool, and (2) the difference in the drywell and wetwell airspace pressures. Upon SRV actuation, pressure builds up inside the piping as SRV blowdown steam compresses the air and forces the water column through the quencher into the suppression pool. The expulsion of water from the SRV line into the suppression pool is called the "water-clearing phase" of the SRV discharge. The loads associated with the water-clearing phase are: (1) transient SRV pipe pressure and thermal loads; (2) pipe reaction forces from transient pressure waves and fluid motion in the pipe; (3) drag loads on structures located in the path of the submerged water jet, and (4) pool boundary loads.

Air follows the water column into the pool in the form of high-pressure bubbles. Once in the pool, the bubbles expand because the ambient pool pressure is lower than the bubble pressure. The subsequent interaction of the air bubbles and the pool water manifests itself as an oscillatory pressure field which persists with decaying amplitude until the air rises to the pool surface. The frequency of the pressure oscillation is influenced by (1) the initial mass of air in the SRV line, (2) the submergence of the SRV discharge line in the pool, (3) the suppression pool temperature, (4) the pool geometry, and (5) the wetwell airspace pressure. Loads associated with the air bubble dynamic phenomena are transient drag loads on submerged structures caused by the velocity field (standard drag) and the acceleration field (inertial drag), and oscillating pressure loads on the pool boundary.

Following the air-clearing phase, steady steam discharge flow is established and continues until the SRV is closed or the reactor is depressurized. The steam enters the pool from the quencher as submerged jets and is completely condensed outside the quencher. Loads associated with the steady steam flow phase of the SRV discharge include (1) pipe reaction forces caused by steady steam flow through pipe bends, (2) thrust forces on the quencher, (3) thermal loads on structures contacted by the steam, and (4) pool boundary loads caused by the oscillation of the condensing steam jets at the quencher.

Following SRV closure, the steam in the discharge line will condense and the resulting vacuum will draw water back into the line. Vacuum breakers on each SRV discharge line are provided to admit drywell air to the discharge line to limit the water reflood rise within the discharge line and allow the water to return to near normal level. This is to prevent large loads during subsequent actuations due to large water leg. Conditions at this time are effectively the same as those prior to actuation, and reopening of the SRV will result in a repeat of the previously described sequence of events. Subsequent actuation of the SRV can influence the magnitude of loads associated with the SRV because the SRV discharge line heated by the previous actuation.

For multiple SRV discharge conditions, the basic discharge line clearing phenomena are the same as for single SRV discharges. The loads on structures in the suppression pool, including

the pool boundary, will be the result of combined effects of the SRV discharge at a number of locations in the suppression pool.

3B.2.2 Loss-of-Coolant Accidents

A spectrum of postulated loss-of-coolant-accidents (LOCAs) is considered to assess the design adequacy of the ABWR containment structure. Each accident condition is described in this section.

3B.2.2.1 Large Break Accident

Two types of large break accidents for the ABWR control the design: the feedwater line break and the main steamline break. In these transients, the upper drywell pressure increases as a result of the mass and energy release from the break, and a steam-air mixture is forced through the drywell connecting vents into the lower drywell. The pressure differential before the pressure is equalized causes a loading on the vessel skirt. Additionally, the flow through the drywell connecting vents causes a drag loading on all structures in those vents.

Concurrent with the air-steam mixture being forced into the lower drywell, the water initially contained in the vent system is accelerated out of the vents. During this vent-clearing process, the water exiting the vents will form submerged jets in the suppression pool which can produce loads on structures near the vent exits and on the suppression pool basemat.

Immediately following the water clearing, bubbles containing air and steam form at the vent exits. As the flow of air and steam from the drywell becomes established in the vent system, the initial bubbles at the vent exits expand with the bubble pressure nearly equal to the drywell pressure. The steam fraction of the flow into the pool will be condensed, but continued injection of drywell air and the resultant expansion of the air bubbles will produce a rapid rise of the suppression pool surface (termed as pool swell). The expanding bubble will cause loads on submerged structures and the suppression pool boundaries.

During the early stages of pool swell, a slug of water is accelerated upward by the expanding air bubbles. Structures and equipment close to the pool surface will experience impact loads as the rising pool surface hits the bottom surface of the structures. Along with these inertial loads, dissipative drag loads will develop as water flows past structures and equipment at elevations above the vent exit and below the maximum pool swell height. These rising and expanding bubbles eventually break through the water ligament and communicates with the wetwell airspace. Breakthrough occurs when the instabilities formed in the rising ligament causes the surface to become unstable and shatter. Froth will continue upward until decelerated to zero velocity by gravity. Because of increasing wetwell airspace pressure, froth would not reach the diaphragm floor, so a pool swell uplift load on the diaphragm floor will not occur.

Following the pool swell transient, a period of high steam flow rate through the vent system will commence. This is followed by a decreasing flow rate as the reactor vessel blowdown

progresses. Prior test data have indicated that the steam will be entirely condensed in the vent exit region.

The steam condensation process is influenced by the vent steam mass flow rate, the subcooling at the vent exit, and the vent flow air content fraction. At medium vent flow rates, the water-to-steam condensation interface will oscillate, causing pressure oscillations in the pool. This phenomenon, referred to as “condensation oscillation”, produces oscillatory and steady loadings potentially severe enough to establish some of the containment design parameters. As the vessel blowdown continues, the vent flow rate will decrease and vent flow air content fraction will become negligibly small. At lower vent flow rates (below a threshold level), the steam bubbles at the vent exit alternately grow, and then nearly instantaneously collapse in a condensation process referred to as “chugging”. This chugging process produces transient dynamic loading on the vents and suppression pool boundary which must be considered in design evaluation of the containment system.

Shortly after a large break accident, the Emergency Core Cooling System (ECCS) pumps will automatically start pumping water from condensate storage pool or suppression pool into the reactor pressure vessel (RPV) to flood the reactor core. Eventually water will cascade into the upper drywell from the pipe break. The time at which this occurs depends on the break size, type, and location. Because the drywell would be full of steam at the time of the vessel flooding, the sudden introduction of water into the drywell will cause condensation of the steam in the drywell and thus depressurization of the drywell. When the drywell pressure falls below the wetwell pressure, the wetwell-to-drywell vacuum breaker (WDVB) system will open vacuum breakers admitting air (noncondensables) from the wetwell airspace to the drywell. This depressurization of the drywell could cause upward loads on the diaphragm floor, whose magnitude would depend on the WDVB system characteristics, and the drywell and wetwell pressure histories. Eventually, a sufficient amount of air will return to equalize the drywell and wetwell pressures.

Following the vessel flooding and drywell-to-wetwell pressure equalization, suppression pool water will continuously recirculate through the reactor vessel via the ECCS pumps. The energy associated with the core decay heat will gradually raise the temperature of the suppression pool. Heat energy is subsequently removed from the suppression pool by the residual heat removal (RHR) heat exchangers. The capacity of the RHR heat exchangers is such that the maximum suppression pool temperature, reached after several hours, remains below the allowable limit. The increase in pool temperature and the corresponding increase in wetwell pressure are considered in the design of the ABWR containment systems.

3B.2.2.2 Intermediate Break Accident (IBA)

The IBA is defined as a break sized such that rapid depressurization of the RPV does not occur due to break flow. However, the reactor inventory loss is sufficiently rapid to cause a reduction in the reactor water level which may have potential for core uncovery. Since the ABWR design

provides three high-pressure ECCSs, the vessel will be flooded without having to depressurize the reactor vessel.

The IBA will increase drywell pressure and temperature at a moderate rate, compared to that due to a large break accident. Water initially contained in the vent system will be accelerated from the vents. During the vent-clearing process, the water exiting the vents will form water jets in the suppression pool, which will cause loads on structures and equipment near the vent exits. The submerged structure loads from an IBA are less severe than those from a design basis accident (DBA). Structures and equipment designed for the DBA water jet loads can readily accommodate the less severe IBA water jet loads.

Immediately following vent water clearing, air and steam bubbles will form at the vent exits. The drywell pressurization rate for an IBA is less than due to an DBA. Consequently, the bubble pressure in the suppression pool is less severe and the moderate rate of drywell pressurization does not result in significant pool swell. The resulting IBA loads on pool boundaries, submerged structures, and equipment are bounded by the corresponding loads from a DBA.

A high drywell pressure signal scrams the reactor during the IBA. The sequence of events following the scram can lead to closure of the main steamline isolation valves (MSIVs) due to low reactor water level. The closure of the MSIVs can result in an increase in RPV pressure, which is relieved by opening of the SRVs. SRV discharge may continue intermittently to regulate reactor pressure and remove decay heat. Consequently, the suppression pool boundary may be subjected to a pressure loading resulting from the SRV discharge during IBA.

For intermediate size breaks, the steam flow rate through the vents may be insufficient to cause condensation oscillation (CO) loads as severe as those during a DBA. Following air carryover, however, chugging loads will be experienced until the reactor vessel blowdown is reduced to a flow rate where chugging becomes inginificant. The subsequent long-term pool temperature transient is essentially the same as that described for the DBA.

3B.2.2.3 Small Break Accident (SBA)

The SBA is defined as an event in which the fluid loss from the RPV is insufficient to either depressurize the reactor or result in a decrease of reactor water level. Following the break, the drywell pressure will slowly increase until the high drywell pressure scram setting is reached. The reactor will scram, but the MSIVs remain open, and close when reactor water level decreases to RPV Level 1.5.

The drywell pressure will continue to increase at a rate dependent on the size of the postulated break. The pressure increase will depress the water level in the vent system until the water is expelled out and air and steam mixture enters the suppression pool. The air flow rate will be such that the air will bubble through the pool without causing any appreciable pool swell. The steam will be condensed and the drywell air will pass through the pool into the wetwell airspace. The wetwell airspace will gradually pressurize at a rate dependent upon the air

carryover rate, which, in turn, depends upon the break size. Eventually, the steam and air flow through the vents will transfer essentially all the drywell air to the wetwell airspace. Following the air transfer, wetwell pressurization will increase at a rate dependent on the rate of increase of the suppression pool temperature.

The vent steam mass flux for an SBA is expected to be insufficient to produce steady condensation oscillation type loading conditions. However, there may be sufficient steam flow rate to cause chugging type of loading conditions. As the RPV depressurizes and cools down, the vent steam mass flux will decrease so that the vents will not remain cleared. Steam condensation will occur at the water interface inside the vents and on the walls of the vent system.

As a result of a postulated MSIV closure, the SRVs will initially discharge to control reactor vessel pressure in response to the isolation transient. Following the initial SRV discharge, SRV cycling will occur at the SRV setpoint pressure. When the temperature of the suppression pool reaches the Technical Specification limit of 48.9 °C during normal operation, the operator will take action to begin a controlled depressurization of the reactor vessel, using manual operation of the SRVs if the MSIVs are closed, or using the main condenser if the MSIVs are open. The rate of depressurization, and thus the total duration of the SBA event, is dependent on operator action. A conservative value for analysis is taken as 56°C/h.

3B.3 Safety/Relief Valve Discharge Loads

During the actuation of a safety/relief valve (SRV), the air initially contained inside the SRV discharge line is compressed and subsequently expelled into the suppression pool by the SRV blowdown steam entering the SRV discharge line. The air exits through holes drilled into an X-quencher device which is attached to the SRV discharge line. The X-quencher discharge device is utilized in the ABWR design to promote effective heat transfer and stable condensation of discharged steam in the suppression pool.

3B.3.1 Quencher Description and Arrangement

The X-quencher discharge device used in the ABWR design is the same as that used in Mark III and Mark II designs. Reference 3B-1 contains a detailed description of design configuration features of the X-quencher discharge device. This discharge device (Figure 3B-2), is a diffuser device comprised of a short conical extension of the vertical terminus of the SRV discharge line and a capped cylindrical central section or plenum, from which four perforated, capped arms extend. The X-quencher, with four arms and many small holes in each arm, directs the air and steam over a broad area. Experimental data (References 3B-2 and 3B-3) have demonstrated the X-quencher characteristics of low air-clearing pressure loadings and no instability in the steam condensation process.

Figure 3B-2 also shows the quencher azimuthal locations in the suppression pool. This arrangement distributes low, intermediate and high pressure-switch set valves uniformly around the pool to preclude concurrent adjacent valves operation.

3B.3.2 Quencher Discharge Loads

3B.3.2.1 Load Definition Methodology

After the air exits into the suppression pool, during the actuation of SRV, the air bubbles coalesce and oscillate as Rayleigh bubbles while rising to the pool free surface. The oscillating air bubbles produce hydrodynamic loads on the pool boundary and drag loads on structures submerged in the pool. After the air has been expelled, steam exits and condenses in the pool. The condensing steam produces negligible (pressure) amplitude loads on the pool boundary, as observed from X-quencher discharge testing.

The methodology for defining the quencher discharge loads (due to initial and subsequent SRV actuations) on the pool boundary for the ABWR containment will be consistent with previously approved methodology for Mark II and Mark III containment designs (NUREG-0802). Reference 3B-4 provides a detailed description of the calculational methodology. This methodology is based directly on empirical correlations obtained from mini-scale, small-scale, and large-scale (including inplant tests) tests conducted to develop a load definition methodology for X-quencher discharge loads during the SRV actuation events.

The X-quencher test data were statistically correlated to calculate the magnitude of quencher air clearing pressure loads on pool boundary as a function of several key parameters. The correlation was developed for use in both Mark II and Mark III containment systems using X-quencher discharge devices for the SRV discharge lines. Detailed descriptions of (1) the database, (2) a quantitative assessment of the test data in terms of the physical phenomena, (3) the procedure for identification and justification of key parameters used in the statistical correlations, (4) the statistical analysis of the data, and the resulting correlation equations, are provided in Section A12 of Reference 3B-1.

In summary, the calculation methodology consists of (1) a statistically derived correlation for predicting the magnitude of the peak positive bubble pressure and a relationship for calculating maximum negative pressure from the maximum positive pressure, (2) an idealized oscillatory pressure history representing subsequent interaction of the quencher air bubble with the suppression pool fluid, (3) a relationship for determining the pressure field in the pool as a function of distance from the quencher, and (4) a technique for determining the total air bubble pool boundary load for subsequent actuation from the first actuation loads, and when more than one quencher bubble exists in the pool (multiple valve actuation conditions).

3B.3.2.2 ABWR Design Quencher Discharge Loads

Quencher discharge pool boundary loads for design evaluation of the ABWR design will be defined after finalization of the ABWR SRV discharge line arrangement layout. After the SRV

discharge line arrangement layout is finalized, the quencher pool boundary design loads will be computed using the methodology described above. The pool boundary pressure $P(r)$ will be calculated from bubble pressure, P_b, using the following relationship:

$$P(r) = \frac{2P_b x r_o}{r} \qquad \text{:for } r > 2r_o \qquad \text{(3B-1)}$$

$$P(r) = P_b \qquad \text{:for } r \le 2r_o \qquad \text{(3B-2)}$$

where

r_o = Quencher radius

r = Line-of-sight distance from quencher center point to the evaluation point (Figure 3B-4)

Air bubble pressure loads from a particular quencher location are considered to act only on boundaries which can be viewed from the quencher bubble with direct line of sight, as illustrated in Figure 3B-5. Figure 3B-6 shows the ideal quencher bubble pressure time history which is normalized with the maximum pressure value. This pressure time history profile will be used in determining pressure amplitude variation with time and the number of pressure cycles. It should be noted that the bubble pressure decay to $1/3P_{max}$ occurs in five cycles for any frequency between 5 and 12 Hz. The justification for this application is from examination of full-scale plant data where most traces were observed to decay to a small fraction of their peak value in two or three cycles.

The design loads will consider and include the following SRV actuation cases:

(1) Single valve discharge for first and subsequent actuations.

(2) Multiple valves discharge.

3B.3.2.2.1 Single Valve Discharge

The most frequent SRV discharge case during the plant lifetime is the single valve discharge of the low setpoint valve.This load case of single valve discharge deals with events such as inadvertent opening of an SRV and actuation of an SRV following small- or intermediate-line breaks in the primary system. A subsequent single SRV actuation may also result to provide pressure relief following a multiple-valve actuation, as described in Subsection 3B.3.2.2.2 below. This actuation, however, involves opening, closing, and reopening of an SRV. Therefore, pressure loading resulting from both first and subsequent SRV actuation will be considered. The SRV line resulting in the most severe pressure loading will be selected for design assessment.

Air bubble pressure loads from a particular quencher (SRV) are considered to act only on boundaries which can be viewed from the quencher bubble with direct line of sight as illustrated in Figure 3B-5, and no load acts on the shaded regions. Load attenuation in the vertical direction will be assumed as shown in Figure 3B-7.

3B.3.2.2.2 Multiple Valves Discharge

This case will cover the events in which all SRVs actuate and the resulting load on the pool boundary will be most severe.Events that are expected to actuate more than one SRV include generator load rejection, loss of main condenser vacuum, turbine trip, closure of all main steam isolation valves, and some less severe transients such as pressure regulator failure and loss of auxiliary power. Some of these anticipated transients may result in actuation of all SRVs. However, variation in time of actuation, valve opening time, and differences in individual discharge line lengths (which influence the time to complete line clearing) will introduce differences in phasing of the oscillating air bubbles in the suppression pool. Air bubbles oscillating out of phase will result in mitigating the pool boundary loads.

The pressure loading for multiple valve discharge will correspond to that resulting from simultaneous first actuation of all SRVs. In view that each SRV has a large value (of about 490 kPa) of blowdown pressure setpoint range, simultaneous subsequent actuation of all SRVs is not expected. Lowest relief set pressure a SRV may cycle and have subsequent actuation to provide pressure relief after multiple valve first actuation. In determining combined pressure loading on pool boundary due to multiple valve actuation, pressure loading due to individual SRV will be assumed equal to the largest of pressure loading calculated for individual valves. Pressure loading due to an individual valve is primarily determined by its relief pressure setpoint and discharge line air volume.The combined pressure loading from multiple valves at an evaluation point will be obtained by SRSS (Square Root of the Sum of Squares) of the individual loads from single valves.

As a bounding and conservative approach for structural evaluation, the multiple valves discharge case will consider and include most severe symmetric and asymmetric load cases. The most severe symmetric load case will assume oscillating air bubbles (from all valves) in phase, and the most severe asymmetric load case will assume one half of oscillating air bubbles 180° out of phase with the other half of oscillating air bubbles. These two load cases will bound all combinations of multiple valve actuation cases.

3B.3.3 Quencher Condensation Performance

After air discharge through the SRV line is completed, steady steam flow from the quencher will be established. Discharged steam condenses in the immediate vicinity of the discharge device. Thermal loads associated with steam jet contact can generally be avoided by appropriate orientation of the discharge device in the suppression pool.

Operating practice of early BWRs, in anticipation that extended SRV steady steam blowdown will heat the pool to a level where the condensation process may become unstable, a

temperature limit for BWR suppression pools was established. This pool temperature limit, specified in NUREG-0783, was established because of concern that unstable steam condensation at high pool temperature could result in high loads on containment structure. Although quencher discharge devices (like the X-quencher) were found to produce smooth steam condensation process, at the time the pool temperature limit was established there were insufficient data available to confirm that quenchers were effective in mitigating loads sue to unstable steam condensation process. NUREG-0783 currently specifies acceptance criteria related to the suppression pool temperature limits for steady state steam condensation condition for the quencher discharge devices.

Recent studies, subsequent to the issuance of NUREG-0783, conclude that steady steam flow through quencher devices (like the X-quencher) is expected to be a stable and smooth condensation process over the full range of pool temperature up to saturation. It is also concluded that the condensation loads for stem discharge less than the loads from equivalent straight pipes. These recent studies are described and discussed in Reference 3B-5.

Subsequent to the studies reported in Reference 3B-5, there were additional test data from quencher discharge tests at high pool temperatures. These tests, reported in Reference 3B-15, showed a long, steady, turbulent, forced plume which consisted of a random two-phase mixture of entrained water and steam bubbles. This additional data, which showed formation of a long continuous steam plume at high pool temperatures, raised an additional concern. It was postulated that large continuous steam plumes may give rise to large bubbles that drift into a cooler region of the pool and suddenly collapse which could transmit significant loads to the pool boundary.

This additional concern was evaluated in a recent study, and i was determined that the continuous plume was not a transient flow shedding large coherent bubbles which might drift away and collapse in a cooler region of the pool. This recent study, described in deal in Reference 3B-16, concludes that the condensation process with SRV dischargers through quenchers (like the X-quencher) into the suppression pool would result in low amplitude loads for all suppression pool temperature.

In view of findings and conclusions from these recent studies discussed in above, it is concluded that suppression pool temperature limits (specified in NUREG-0783) for SRV discharge with quenchers are no longer necessary. Therefore, given that the ABWR design utilizes X-quencher discharge devices, the pool temperature limit specified in NUREG-0783 were not considered. However, ABWR design retains the restrictions on the allowable operating temperature envelope of the pool, similar to those in place for operating BWRs.

Further, the studies in Reference 3B-5 conclude that steam condensation loads with X-quenchers over the full range of pool temperature up to saturation are low compared to loads due to SRV discharge line air clearing and LOCA events. Therefore, considering that ABWR design considers SRV air Clearing and LOCA steam condensation loads for containment

design evaluation, dynamic loads during the quencher steam condensation process will not be defined and considered for containment design evaluation.

3B.4 Loss-of-Coolant Accident Loads

In this section, methodologies for calculating the dynamic loading conditions associated with the various LOCA phenomena are presented.

3B.4.1 Pressure and Temperature Transients

A LOCA causes a pressure and temperature transient in the drywell and wetwell due to mass and energy released to the drywell. The severity of this transient loading condition depends upon the type and size of LOCA. Section 6.2 provides pressure and temperature transient data in the drywell and wetwell for the most severe LOCA case [design basis accident(DBA)]. This transient data establish the structural loading conditions in the containment.

3B.4.2 Vent Clearing and Pool Swell Loads Methodology

Following a postulated DBA, the drywell pressurizes and the water in the vents is expelled out into the suppression pool. The water forms jets in the suppression pool which induce loads on structures near the vent exits. After the water is cleared from the vents, the air in the vents and the drywell flows into the suppression pool. Air bubbles form at the vent exits, expand under the pool surface, and produce pressure loading on the suppression pool boundary. The expansion of the air bubble forces the slug of water above the bubbles to accelerate upward (pool swell), which causes both impact and drag loads on structures within the swell zone. Upon reaching the maximum swell height, the air bubbles that drive the water slug penetrates through the surface, resulting in froth formation. This froth will impact structures located above the maximum bulk swell height. The froth created after breakthrough experiences gravity-induced phase separation and will fallback toward the pool bottom. During this fallback, structures will be subjected to fallback drag loads.

Consistent with the load definition methodology for Mark I, II and III containments, sonic and compression wave loadings, occurring immediately following the postulated instantaneous rupture of a large primary system pipe, will not be considered and defined for design evaluation of the containment structure. It was concluded that these waves would result in a negligible structural response.

3B.4.2.1 Pool Boundary Loads

Following a postulated LOCA and after the water is cleared from the vents, air/steam mixture from the drywell flows into the suppression pool creating a large bubble at vent exit as it exits into the pool. The bubble at vent exit expands to suppression pool hydrostatic pressure, as the air/steam mixture flow continues from the pressurized drywell. Water ligament above the expanding bubble is accelerated upward by the difference between the bubble pressure and the

air space pressure above the pool. This acceleration of water ligament gives rise to pool swell phenomena, which, typically, lasts for a couple of seconds.

During this pool swell phase, wetwell region is subjected to the hydrodynamic loading conditions, and they are:

- Loads on suppression pool boundary and drag loads on structures initially submerged in the pool, due to the pressurized and expanding bubble at vent exit
- Loads on wetwell airspace boundary (including the diaphragm floor), due to rising pool which compresses the wetwell air space
- Impact and drag loads on structures located above the initial pool surface, due to the rising pool surface

From a structural design standpoint, the most important aspects of the pool swell phenomena are peak pool swell height and peak pool swell velocity. The former determines a region of impact/drag loading condition, whereas the latter determines severity of the loading condition.

ABWR Pool Swell Loads

ABWR pool swell response calculations to quantify pool swell loads were based on a simplified, one dimensional analytical model. The model was qualified against test data from the Pressure Suppression Test Facility (PSTF) for a 1/3 - scaled Mark III pressure suppression system geometry. The methodology is similar to that reviewed and accepted by the staff (NUREG-0808) for application to Mark II plants. The ABWR pressure suppression system design is similar to the Mark III design. The main difference is the smaller gas space above the suppression pool in the ABWR. This difference is accounted for in the analytical model for the pressure suppression system.

Model Vs. Mark III Horizontal Vent Test Data

Test data used to qualify the analytic model was taken from 1/3-scale tests for a Mark III geometry. The submergence to pool width ratio was representative of conditions in an ABWR. The GOTHIC code was used to model the Mark III tests. The model was designed to bound the test data. The test data used in the model comparison, and the modeling approach are fully described in Reference 3B-17. The major modeling assumptions were:

- The wetwell is represented by a subdivided one-dimensional model.
- The drywell pressure transient was specified using data from the tests.
- Pressure losses between the measured pressure in the drywell and the weir wall region were ignored to maximize the air flow into the suppression pool.
- A single horizontal vent, having the full combined open area of the three horizontal vents, was modeled at the elevation of the top vent.

Comparison results, summarized in Reference 3B-17 demonstrate and assure adequacy of the model for calculating ABWR pool swell response.

Pool Swell Loads

Pool swell response calculations were done using the same modeling approach and assumptions that were used in the qualification against the 1/3 scale Mark III test data. The model is fully described in Reference 3B-17.

The model includes:

(1) Noncondensable gases are assumed to behave as an ideal gas.

(2) After the vent clearing, only noncondensable gases flow through the vent system.

(3) The flow rate of noncondensable gases through the vent system is calculated assuming one-dimensional flow with possible choking at the vent exit.

(4) All three horizontal vents are combined into a single flow path that has the total flow area of all three vents. The bottom of the single modeled vent is located at the physical bottom of the top vent in the vertical vent pipe.

(5) The temperature of bubbles is forced to near thermal equilibrium with the pool.

(6) The built-in interfacial drag models in GOTHIC are used to predict the bubble expansion and the acceleration of the water above the vents, including differential velocity in the air and water phases resulting in thinning of the slug as it rises.

(7) Friction between pool water and the pool boundaryis neglected.

(8) Noncondensable gas in the wetwell airspace is compressed by the rising water. For predicting the maximum slug velocity, the air space is assumed to be in thermal equilibrium with the pool to minimize the air space pressure. For predicting the maximum bubble and air space pressure, the air space is assumed to be thermally isolated from the pool.

(9) Heat transfer to the pool and air space boundaries is ignored.

(10) The air bubble is constrained to rise in an area that is 80% of the full pool area.

The calculated pool swell loading conditions for the ABWR containment system obtained from the analytical model (identified above) and the above modeling assumptions are shown in Table 3B-1.

Pool boundary pressure distribution is shown in Figure 3B-11, and pressure time history of air bubble pressure is shown in Figure 3B-12.

Figure 3B-13 shows types of loading regions for structures located above the initial pool surface during the pool swell phase of LOCA. Key structures that will be subjected to these loads are: SRV discharge piping; catwalk structure; wetwell-to-drywell vacuum breakers.

Structures located between 0 and 8.8m above the initial surface will be subjected to impact load by an intact water ligament, where the 8.8m value corresponds to the calculated maximum pool swell height. The load calculation methodology will be based on that approved for Mark II and Mark III containments (NUREG-0487 and NUREG--0978).

Structures located at elevations between 8.8m and 12.1m will be subjected to froth impact loading. This is based on the assumption that bubble breakthrough (i.e., where the air bubbles penetrate the rising pool surface) occurs at 8.8m height, and the resulting froth swells to a height of 3.3m. This is considered to be a conservative value for the ABWR containment design. Because of substantially smaller wetwell gas space volume (about 1/5th of the Mark III design), the ABWR containment is expected to experience a froth swell height substantially lower than that in Mark III design. The wetwell gas space is compressed by the rising liquid slug during pool swell, and the resulting increase in the wetwell gas space pressure will decelerate the liquid slug before the bubble break-through process begins. The load calculation methodology will be based on that approved for the Mark III containment (NUREG-0978).

As shown in Figure 3B-13 the gas space above the 12.1m elevation will be exposed to spray condition which is expected to induce no significant loads on structures in that region.

As drywell air flow through the horizontal vent system decreases and the air/water suppression pool mixture experiences gravity-induced phase separation, pool upward movement stops and the “fallback” process starts. During this process, structures between the bottom vent and the 12.1m elevation can experience loads as the mixture of air and water fall past the structure. The load calculation methodology for defining such loads will be based on that approved for Mark III containment (NUREG-0978).

3B.4.2.2 Loads on Access Tunnel

The ABWR design provides two access tunnels through the suppression chamber for access from the reactor building to the lower drywell. These tunnels provide access for personnel and equipment, and the bottom of these two tunnels is partially submerged when suppression pool water is at its nominal level position. During pool swell, the access tunnel will be subjected to drag load only. Because of their initial partial submergence, the tunnels are not expected to experience any impact load due to pool swell.

The drag load imposed on the access tunnel due to pool swell will be calculated by the following equation:

$$P_d = 1/2 C_d \zeta \frac{V_{Max}^2}{g_c} \quad \text{(3B-3)}$$

where

P_d = Drag pressure load

C_d = Drag coefficient

V_{Max} = Maximum pool swell velocity

ζ = Density of water

g_c = Conversion constant

The drag coefficient, C_d, will be determined from Figure 3B-14. The maximum velocity, V_{Max} in the above equation will be 1.1 times the maximum vertical velocity calculated from the pool swell analytical model.

The pressure loading due to air bubble pressure will be calculated and added to the drag load. This pressure loading will consider and account for the wetwell airspace pressure as shown below:

$$P_b = P_B - P_{w/w} \quad \text{(3B-4)}$$

where

P_b = Net pressure loading due to air bubble pressure

P_B = Air bubble pressure

$P_{w/w}$ = Wetwell airspace pressure

In addition to the drag and air bubble pressure loading, the access tunnel will also be subjected to buoyancy loading, as shown by the following equation:

$$P_{by} = \frac{\zeta V_T}{A} \quad \text{(3B-5)}$$

where

P_{by} = Pressure loading due to buoyancy

ζ = Density of water

V_T = Displaced volume of access tunnel

A = Projected area of access tunnel

3B.4.2.3 Impact and Drag Loads

As the pool level rises during pool swell, structures or components located above the initial pool surface (but lower than its maximum elevation) will be subjected to water impact and drag loads. The following equations will be used to compute the applicable impact and drag loads on affected structures.

Impact Load

The impact loading on structures between initial pool surface and the maximum swell height due to pool swell will be calculated by the following equation:

$$P(t) = P_{Max}\frac{(1 - Cos(2\pi t/T))}{2} \quad (3B\text{-}6)$$

where

$P(t)$ = Pressure acting on the projected area of the structure

P_{Max} = The temporal maximum of pressure acting on projected area of the structure

t = Time

T = Duration of impact

For both cylindrical and flat structures, the maximum pressure P_{Max} and pulse duration T will be determined as follows:

(a) The impulse will be calculated using the equation given below:

$$I_P = \left(\frac{M_H}{A}\right)\frac{V}{gc} \quad (3B\text{-}7)$$

where

I_P = Impulse per unit area

$\left(\frac{M_H}{A}\right)$ = Hydrodynamic mass per unit area

V = Impact velocity

gc = Conversion Constant

(b) The hydrodynamic mass per unit area for impact loading will be obtained from the appropriate correlation for a cylindrical or flat target from Figure 6-8 of Reference 3B-6.

(c) The pulse duration T will be obtained from the following equation:

Cylindrical Target:

$$T = (0.0463 \times D)/V \quad \text{(3B-8)}$$

Flat Target:

$T = (0.011 \times W)/V$ for $V \geq 2.13\,m/s$

$= (0.0052 \times W)$ for $V < 2.13\,m/s$

where

T = Pulse duration, s

D = Diameter of cylindrical pipe, m

W = Width of the flat structure, m

V = Impact velocity, m/s

(d) The value of P_{Max} will be obtained using the following equation:

$$P_{Max} = (2I_P)/T \quad \text{(3B-9)}$$

For both cylindrical and flat structures, a margin of 35% will be added to the P_{Max} values (as specified above) to obtain conservative design loads.

Drag Load

Following the impact loading, the structure above the initial pool surface (but below the maximum swell height) will be subjected to the standard drag loading. This drag loading will be calculated using the methodology described in Subsection 3B.4.2.2.

$$P_d = 1/2 C_d \zeta (V^2/g_c) + V_A \zeta (\dot{V}/g_c) \quad (3B\text{-}10)$$

where

P_d = Drag pressure

C_d = Standard drag coefficient

V = Pool swell velocity

ζ = Density of water

g_c = Conversion constant

V_A = Acceleration drag volume

$\dot{V}$ = Pool acceleration

The standard drag coefficient, C_d, in the above equation and acceleration drag volume, V_A, will be used consistent with those defined and used in Reference 3B-1. The time history of pool swell velocity will be calculated from the analytical model described in Subsection 3B.4.2. The pool swell velocity calculated from the analytical model will be multiplied by a factor of 1.1 (for conservatism) for application in calculation of the drag load. Time history of pool swell surface level will be determined from the same analytical model used for pool swell velocity calculation. The pool swell acceleration, $\dot{V}$, will be computed from the pool swell velocity data.

3B.4.2.4 Loads on Diaphragm Floor

Rapid pressurization of the wetwell airspace during the pool swell transient has a potential for upward differential pressure loading on the diaphragm floor. Results from the pool swell analytical model, however, showed that wetwell airspace pressure did not exceed the drywell pressure during the pool swell transient. Hence, it is concluded that the diaphragm floor will not be subjected to an upward differential pressure loading. The diaphragm floor will be subjected to only downward differential pressure loading, during the pool swell phase.

3B.4.3 LOCA Steam Condensation Loads

3B.4.3.1 ABWR Horizontal Vent Test Program

LOCA loads with the horizontal vent system design have been well characterized during the Mark III Confirmatory Test Program. More than 200 tests have been performed to determine horizontal vent system performance and associated LOCA loads. However, all of these tests have utilized the low containment pressure characteristics of the Mark III containment system (about 34.32k Pa G). Because of some thermodynamic and geometrical differences between the ABWR and Mark III designs, it was anticipated that condensation oscillation (CO) and chugging (CH) loads might differ from prior (Mark III) testing in horizontal-vent facilities. These included (1) increased ABWR wetwell airspace pressure, and hence subcooling, (2) the presence of a lower drywell (L/D), (3) the smaller number of vents (30 in ABWR vs. 120 in Mark III), (4) extension of the vents in the pool, (5) vent submergence, and (6) suppression pool width.

Considering the existence of the above thermodynamic and geometrical differences, a test program was conducted to confirm the CO and CH loads which would occur in the event of a LOCA in an ABWR plant. The test program, test data, and interpretation of test data are documented in Reference 3B-7.

The test program consisted of 24 simulated blowdowns (Table 3B-2) in test facilities representing the horizontal-vent ABWR design. The tests were divided into two parts utilizing sub-scale (SS) and partial full-scale (FS^*) test facilities shown in Figures 3B-15 and 3B-16, respectively. Figures 3B-17 and 3B-18 show test sensors common to FS^* and SS tests, and unique to FS^* and SS tests, respectively.

The SS facility had all linear dimensions reduced by a factor of 2.5 from prototypical ABWR dimensions. Thirteen SS tests were performed primarily for the purpose of obtaining CO data. A full-scale vertical and horizontal-vent configuration was installed for the FS^* tests. The upper drywell (U/D) was enlarged but not to prototypical dimensions. Eleven FS^* tests were performed primarily for the purpose of obtaining CH data. The test matrix for the 24 blowdowns (Table 3B-2) included variations in pool temperature, break size, wetwell backpressure, and type of break (steam or liquid). The test facilities were equipped adequately with the data sensors to obtain necessary data for understanding the phenomena and establishing a database for defining CO and CH loads for the ABWR containment. In addition to the geometrical considerations, the facility was designed to minimize the potential for fluid-structure interaction (FSI). Measurements were taken at seven locations on the wetted suppression pool boundary to record dynamic pressure oscillations. Structural instrumentation (strain gauges and accelerometers on the basemat, pedestal, and containment walls) was used to confirm that FSI effects were minimal. Pressure transducers in the vertical and horizontal vents recorded dynamic loads on the vent system.

Loads due to condensation oscillation and chugging are described and discussed in Subsections 3B.4.3.2 and 3B.4.3.3, respectively.

3B.4.3.2 Condensation Oscillation (CO) Loads

The condensation oscillation (CO) period of a postulated LOCA follows the pool swell transient. During the CO period, both the vent steam mass flux and vent air content are decreasing. The steam-water interface at the vent exit oscillates as the steam is condensed. The vent steam mass flux is sufficient to prevent water flow into the vent. The steam condensation process at the vent exit induces pressure loads on the containment system, including the suppression pool boundaries and structures submerged in the suppression pool.

3B.4.3.2.1 Description of CO Database

A detailed description, evaluation, and discussion of CO data are given in Reference 3B-7.

The test program consisted of a total of 13 simulated blowdowns in sub-scaled test facility representing a one-cell (36°) sector of the ABWR horizontal vent design, which included a single vertical/horizontal vent module. The subscaled (SS) test facility was geometrically (all liner dimensions scaled by a factor of 2.5) similar to the prototypical ABWR design, and the single vertical/horizontal vent module included all three horizontal vents, as shown in Figure 3B-15. In these tests, full-scale thermodynamic conditions were employed. This approach is based on the belief that condensation phenomena at the vent exit are mainly governed by the thermodynamic properties of the liquid and vapor phases. In accordance with this scaling procedure, measured pressure amplitudes are equal to full-scale values at geometrically similar locations, whereas measured frequencies are 2.5 times higher than the corresponding full-scale frequencies.The technical basis for using this scaling approach was based on extensive review and evaluation of the available literature on CO scaling and scaled tests performed for Mark II and Mark III containments, as well as general consensus of technical experts in this field. The CO scaling studies, which have been performed independently by various technical experts, show that for tests in a geometrically scaled facility with full-scale thermodynamic conditions, the measured pressure amplitudes are the same as full-scale values at geometrically similar locations, and measured pressure frequencies are the scale factor times higher than the corresponding full-scale frequencies.

Therefore, CO frequencies for the full-scale ABWR design are obtained by scaling the frequencies measured in SS tests by a factor of 2.5. A similar technique is applicable to scaling adjustment in frequency for obtaining full-scale values. Thus, this scaling procedure made it possible to use the measured SS data (pressure time history) directly for load definition purpose after the time scale is compressed by a factor of 2.5.

Out of the 13 SS tests, the tests recommended for definition of the CO load are SST-1, 2, 3, 9, 11, and 12. These six tests, summarized in Table 3B-2, were run at prototypical conditions. Of the remaining tests, SST-4, 5, 6, 7, 8, and 14 were run with a prepurged vent system, and SST-10 was run with the L/D blocked off. These tests are valuable for understanding CO phenomena

and the effects of system variables, but they are not considered to be an appropriate basis for the CO load definition.

3B.4.3.2.2 Evaluation of CO Database

Each of the CO load definition tests shows significant frequency peaks at 5 and 9 Hz. Figure 3B-19 (solid curve) illustrates this behavior at the basemat (019P) sensor location. The 9 Hz frequency corresponds to a full-scale CO driver frequency near 4 Hz, which is representative of diameter at vent exit. The lower frequency is associated with the vent acoustic frequency which is representative of drywell-to-wetwell connecting vent.

Examination of the data in Figure 3B-20 shows that, in general, the largest amplitude loads occurred at transducer location 019P (on basemat, near pedestal wall), and that the loads increased with increasing break size and increasing pool temperatures.

Figure 3B-19 shows the comparison between the pressure oscillation power spectral density (PSD) from the small-scaled test and pressure oscillation analysis from design source. The analysis PSD envelopes the test data PSD.

3B.4.3.2.3 CO Load Definition

The load definition methodology for the design CO load for the ABWR containment uses a source load approach which is described in the following subsections. In development of this methodology, all pertinent data from Mark II and Mark III tests were reviewed and considered.

3B.4.3.2.3.1 Source Load Approach

For prior BWR containments, the CO loading is defined and applied as a rigid-wall load at the fluid-structure interface. This application of the CO loading to a coupled containment model can produce relatively large structural responses, since the pressure oscillation frequencies are close to the natural frequencies of the fluid-structure system.

An alternate formulation of the CO load, termed as “Source Load Approach”, is to develop a source load. The source load is a series of pulses which simulates the oscillation of the steam/water interface at the horizontal vent exits. This approach has recently been used successfully for BWR containments. In this approach the CO source load would be applied to a coupled fluid-structure model of the ABWR containment as an excitation of the steam/water interface at the exits of the horizontal vents. It is the oscillatory motion of the steam/water interface which produces the characteristic oscillatory pressure loading on the wall. With a source load, it will be possible to account for the spatial distribution of the load and the variation of pool and vent fluid properties in a natural way. This approach avoids the problem of artificial resonant amplification at the system frequencies.

Figure 3B-21 describes the CO source load methodology. In order to develop a technically justified source loading function, the methodology includes the following elements:

(1) A comprehensive test database

(2) A coupled steam-water-structure interaction model of the test facility from which the data were obtained

(3) A procedure to develop a “test source” loading configuration

(4) A criteria to evaluate the test source loading configuration and test facility model

(5) A procedure to scale up the test source to a full-scale design source for the ABWR containment system

(6) A full-scale coupled steam-water-structure interaction model of the ABWR containment system

(7) A criteria to evaluate the design source loading condtion for the ABWR containment system

(8) Calculation of CO design (wall pressure) from the ABWR analysis using the design source

Criteria for CO Source Load

An acceptance criterion is specified in order to provide a basis for judging the acceptability of the source loading function with respect to prediction of wall pressure loadings and their frequency contents. The criteria include the following elements:

(1) Wall pressure histories for the SS test facility produced by the test source match with the pressures measured in the SS test facility.

(2) Frequency content of the predicted pressure histories, as defined by a power spectral density (PSD) and by an amplitude response spectrum (ARS), matches with the data obtained from the SS test facility.

(3) Spatial distribution of the root mean square (RMS) of the predicted loading matches with the data measured from the SS test facility.

(4) Wall pressures predicted by the design source for the full-scale (ABWR) facility match with the pressures measured in the SS test facility at geometrically similar locations. Note, this is required by the CO scaling laws (References 3B-8 and 3B-9).

Figure 3B-22 shows pressure time history representative of ABWR CO load determined using the source load approach described above.

The higher amplitudes in ABWR can be attributed to a deeper submergence in ABWR (3.5m vs. 2.3m), and the fact that in ABWR tests all three horizontal vents remained open during the maximum CO period whereas in Mark III tests the bottom and middle vents were closed at the onset of CO conditions. There may be some partial contribution from increasing wetwell overpressure during CO period in ABWR tests.

Load Application Methodology

For design evaluation of containment structure, the pool boundary pressure loads obtained from analysis of single-vent (36°) model of the prototypical ABWR design were specified and applied over the full (360°) model of the ABWR configuration. This CO loading specification implies all vertical vents are in phase (i.e., no credit for phasing among vents), which is considered to be a conservative load definition approach.

3B.4.3.3 Chugging Loads

Chugging, a hydrodynamic phenomenon associated with a LOCA, follows the CO period and occurs during periods of low vent steam mass flux and, typically, produces a sharp pressure pulse followed by a damped oscillation. During chugging, rapid steam condensation causes the pool water to re-enter the vents. This is followed by a quiescent period until the steam-water interface is forced out into the pool. Thus, chugging, an intermittent event, is the result of unsteady condensation occurring in the last stages of the blowdown. As stated earlier, specific tests were conducted to obtain chugging data for defining the chugging loads for the ABWR containment system.

3B.4.3.3.1 Description of Chugging Data

As shown in Table 3B-2 under the FS* part of the Horizontal Vent Test (HVT) matrix, 11 tests were performed primarily for the purpose of establishing a database for definition of the CH load for ABWR design evaluation. The HVT facility for the FS* test series was run with a full-scale vertical vent and horizontal vent system and an enlarged U/D. The tests were run at prototypical mass flux and pool temperature and with the vent system purged of air. It is known from previous blowdown testing and observations that presence of air in the vent reduces CH loads, so running chugging tests at prepurged conditions is conservative.

3B.4.3.3.2 Evaluation of Chugging Data

A detailed description and discussion of chugging data are contained in Reference 3B-7.

A typical large chug from the full-scale database is shown in Figure 3B-24 and its PSD in Figure 3B-25. It is characterized by a small underpressure, followed by a positive pressure pulse, and a decaying ringout. These phenomena are associated with the initial contraction of the steam bubble, the rapid deceleration of pool water converging on the vent exit, and the excitation of an acoustic standing wave in the pool. Chugging data from Mark II and Mark III testing also exhibited similar characteristic features.

Figure 3B-23 shows the dependence of chugging loads on suppression pool temperature. This amplitude data clearly show that the most severe chugging occurs for the steam breaks with an initial pool temperature of 21°C. Chugging loads decrease significantly as the pool temperature is raised to 49°C. In general, the data support the understanding (observed from prior tests) that chugging has some dependence on system parameters, such as mass flux and pool temperature, along with a substantial degree of randomness.

3B.4.3.3.3 Chugging Load Definition

Figure 3B-26 shows various elements of the source load methodology for defining the chugging load on the pool boundary. The database consisted of 11 tests conducted in the HVT facility with the full-scale vent system. From this database, key chugs were selected which serve as criteria for the development of the source load. The key-chug approach was used successfully for the definition of the Mark II chugging load (Reference 3B-10).

Key chug selection was determined by requiring that the PSD envelope of the selected key chugs matches the PSD envelope of the FS* chugging database. The criterion for a technically justifiable chug design source is that the design source load, when applied to an analytical model of the HVT facility, produces a wall pressure which matches the selected data and a PSD envelope which envelopes the PSD envelope of the selected data.

3B.4.3.3.3.1 Pool Boundary Loads

Eight different chugging design sources, represented by a single pulse acting at the exit of top vent in a full-scale model, were defined. The design sources were determined by imposing a requirement that the PSD envelope generated by these design sources bounds the PSD envelope from the selected chugging data. A comparison of PSD results from analysis and test data (for sensor location 019P) is shown in Figure 3B-27. Figure 3B-28 shows spatial distribution of maximum pool boundary pressure. For design evaluation of affected structures, a total of eight pressure time histories, corresponding to eight design sources, will be computed and specified. A typical pressure time history at the bottom pool boundary is shown in Figure 3B-29 which will form the basis for the spatial distribution shown in Figure 3B-28.

Load Application Methodology

The pool boundary pressure loads obtained from analysis of a single-vent (36°) sector model of the prototypical ABWR design were specified for application over the full (360°) model of the prototypical ABWR facility. To bound symmetric and asymmetric loading conditions, two load cases were defined.

Case 1: All vents chugging in phase.

Case 2: Vents in one half chugging 180° out of phase with the other half vents

3B.4.3.3.3.2 Loads on Access Tunnel

The bottom of the access tunnel is treated as a wetted boundary at the top of the top pool surface. The axial and circumferential pressure loadings on the submerged portion of the access tunnel are as shown in Figures 3B-28 and 3B-30, respectively. The pressure attenuation in the axial direction is assumed to vary linearly from the pedestal to the opposite containment wall, and the circumferential attenuation on the tunnel perimeter is assumed to vary with the submergence.

3B.4.3.3.3.3 Loads on Horizontal Vent

The HVT FS facility was instrumented with two load cells on the top horizontal vent to measure the vertical force and bending moment experienced by the vent during chugging. Steam bubble collapsing inside the vent has a potential to induce significant loading on the horizontal vent. With the ABWR vent system design, in which the horizontal vents project into the pool, it is anticipated that these may be significant for structure evaluation.

Typical test results from the HVT program are exhibited in Figure 3B-31.

For structure evaluation of the horizontal vent pipe and pedestal, an upward load, based on the HVT test data, is conservatively defined as shown in Figure 3B-33.

For building structure response analysis for the evaluation of RPV and its internals, the horizontal vent upward load is specified as shown in Figure 3B-34. To bound symmetrical and asymmetrical loading conditions, the following two load cases will be considered and analyzed.

(1) Upward load on the pedestal wall simultaneously at all top 10 horizontal vents

(2) Upward load on the pedestal wall simultaneously at top five vents in one-half side of pedestal

3B.4.4 RCIC Turbine Exhaust Steam Condensation

The Reactor Core Isolation Cooling (RCIC) system, which forms part of the Emergency Core Cooling Systems (ECCS), will maintain sufficient reactor water inventory in the event that the reactor vessel is isolated and the feedwater supply unavailable. The RCIC system injects water into a feedwater line, using a pump driven by a steam turbine. The steam turbine is driven with a portion of the decay heat steam from the reactor vessel and the turbine exhaust steam is piped into the suppression pool where it is condensed. The RCIC system is designed to perform its intended function without AC power for at least 2 hours with a capability up to 8 hours.

In view that the turbine steam discharges and condenses in the suppression pool and the expected long duration of RCIC operation, there exists a potential for steam condensation loading on the pool boundary. Significance of such potential loading on the pool boundary (steel liner, in specific) was examined, and it was determined that this loading condition will be well bounded by the LOCA steam condensation design loads.

3B.4.4.1 Exhaust Steam Condensation Loading

The RCIC system is a safety system, consisting of a steam turbine, pump, piping, accessories, and necessary instrumentation. To minimize exhaust steam line vibration and noise levels, the discharge end of the turbine exhaust line will be equipped with a condensing sparger. The sparger design configuration will be similar to that currently used successfully for the operating BWRs. The turbine exhaust piping, including the RCIC sparger, is designed to retain piping pressure integrity and functional capability.

The condensing sparger is expected to produce a very smooth steam condensation operation resulting in low pressure fluctuations in the pool, which would imply low pressure on the pool boundary. During the extended RCIC operation, condensing exhaust steam will bring the pool to high temperature. At high pool temperatures, long plumes consisting of a random two-phase mixture of entrained water and steam bubbles are expected to exist. As reported in Reference 3B-16, this plume would not shed large coherent bubbles. Large coherent bubbles are a concern because they may drift and collapse in a cooler region of the pool, potentially producing significant loads to the pool boundary.

Therefore, in view of above, steam discharge through the condensing sparger is expected to be a smooth condensation process which would result in low pressure fluctuation loading on the pool boundary. This expected asymmetric loading condition, which is expected to be a low pressure fluctuation loading, should be bounded by the LOCA steam condensation (CO and Chugging) loads defined for the ABWR design. Further, the ABWR design load definition specifies a bounding asymmetric load case which assumes vents in one half chugging 180° out of phase with the other half vents. This is a conservative representation of asymmetric loading.

In summary, it is concluded that steam condensation loads associated with the RCIC turbine exhaust steam discharge (via condensing sparger) to the pool will produce low pressure fluctuation loads on the pool boundary. Such loads should be well bounded by the LOCA steam condensation loads. The turbine exhaust piping, being designated as ASME Class 2 piping, shall be designed to retain its pressure integrity and functional capability.

3B.5 Submerged Structure Loads

Structures submerged in the suppression pool can be subjected to flow-induced hydrodynamic loads due to LOCA and SRV actuations.

During a LOCA, steam/water mixture rapidly escapes from the break, and the drywell is rapidly pressurized. The water initially in the vent system is expelled out into the suppression pool. A highly localized induced flow field is created in the pool and a dynamic loading is induced on submerged structures. After the water is expelled from the vent system, the air initially in the drywell is forced out through the horizontal vents into the suppression pool. The air exiting from the vents forms expanding bubbles which create moderate dynamic loads on structures submerged in the pool. The air bubbles cause the pool water surface to rise until they break

through the pool water surface. The pool surface water slug decelerates and falls back to the original pool level. Steam/water mixture from the break soon fills the drywell space and is channeled to the pool via the vent system. Steam condensation starts and the vibratory nature of pool water motion causes an oscillatory load on submerged structures.

The CO loading continues until the pressure in the drywell decreases. This is followed by a somewhat regular but less frequent vibration called chugging (CH). During the CH period, a high frequency spike is propagated, which causes an acoustic loading on submerged structures.

During SRV actuations, the dynamic process of the steam blowdown is quite similar to LOCA steam blowdown but the induced load is mitigated by the X-quencher device attached at the end of each discharge line. Two types of loads are important. One is due to the water jet formed at the confluence of the X-Quencher arms and another is due to the four air bubbles formed between the arms of the X-Quencher. These air bubbles are smaller in size than the LOCA air bubbles, reside longer in the pool, and oscillate as they rise to the free surface of the pool.

Key submerged structures that will be subjected to significant loads due to LOCA (pool swell, CO, CM) and SRV actuation events are:

- Submerged portion of SRV discharge lines
- SRV discharge line X-quencher discharge device and its support structure
- Personnel and equipment access tunnels (partially submerged)
- ECCS suction lines and strainers.

3B.5.1 Pool Swell Submerged Structure Loads

During the initial phase of the DBA, the drywell airspace is pressurized and the water in the vents is expelled to the pool and induces a flow field throughout the suppression pool. This induced flow field is not limited to direct jet contact and creates a dynamic load on structures submerged in the pool.

However, since none of the submerged structures in the ABWR containment is in the direct path of these jets, the dynamic load on these structures is less than the load induced by the LOCA air bubble that forms after the water is expelled out. Since the air bubble induced dynamic load is bounding, this load is conservatively used in place of water jet load.

After the vents are cleared of initially contained water, pressurized drywell air is purged into the suppression pool, and a single bubble is formed around each vent exit. It is during the bubble growth period that unsteady fluid motion is created within the suppression pool. During this period, all submerged structures below the pool surface will be exposed to transient hydrodynamic loads.

The load definition methodology for defining the LOCA bubble-induced loads on submerged structures will be consistent with the methodology used for prior plants, as described in Reference 3B-11.

3B.5.2 Condensation Oscillation Submerged Structure Loads

During a LOCA, after the vent is cleared of water and the drywell air has been carried over into the wetwell, steam condensation begins. This condensation oscillation phase induces bulk water motion and, therefore, creates drag loads on structures submerged in the pool.

The load definition methodology for defining the LOCA steam condensation oscillation loads on submerged structures will be consistent with the methodology used for prior plants. The methodology is described in Reference 3B-12.

3B.5.3 Chugging Submerged Structure Loads

Chugging occurs after drywell air has been purged and carried over into the wetwell, and the vent steam mass flux falls below a critical value. Chugging then induces acoustic pressure loads on structures submerged in the pool.

The load definition methodology for defining the LOCA chugging loads on submerged structures will be consistent with methodology used for prior plants. The methodology is described in Reference 3B-12.

3B.5.4 SRV Submerged Structure Loads

Following the actuation of a SRV, water contained initially in the discharge line is rapidly discharged through the X-Quencher discharge device attached at the end of the SRV discharge line. A highly localized water jet is formed around the X-Quencher arms. The hydrodynamic load induced outside a sphere circumscribed around the quencher arms by the quencher water jet is not significant. There are no submerged structures located within the sphere mentioned above in the ABWR arrangement. The induced load for submerged structures located outside the circumscribed sphere by the quencher arm is negligible and is ignored.

After the water discharge, the air initially contained in the discharge line is forced into the suppression pool under high pressure. The air bubbles formed interact with the surrounding water and produce oscillating pressure and velocity fields in the suppression pool. This pool disturbance gives rise to hydrodynamic loads on submerged structures in the pool.

The load definition methodology for defining the SRV air bubble loads on submerged structures will be consistent with that used for prior plants. The methodology is described in References 3B-11 and 3B-13.

3B.6 Loads Combination

Under certain plant conditions, the containment structures can be subjected simultaneously to hydrodynamic loads due to LOCA and SRV actuations. Event-time relationships showing load combination histories for design assessment of the ABWR containment system will be, in general, consistent with the approach used for prior plants. If found necessary, any ABWR-unique features will be considered and addressed appropriately.

3B.7 References

3B-1 General Electric Company, "Containment Loads Report (CLR), Mark III, Containment", 22A4365AB, Rev. 4, Class III, January 1980.

3B-2 General Electric Company, "Caorso SRV Discharge Tests Phase I Test Report", NEDE-25100-P, May 1979.

3B-3 General Electric Company, "Caorso SRV Discharge Tests Phase II ATR", NEDE - 25118, August 1979.

3B-4 GESSAR II, Appendix 3B, Attachment A, 22A7007, 1984.

3B-5 General Electric Company, "Elimination of Limit on BWR Suppression Pool Temperature For SRV Discharge With Quenchers", NEDO - 30832, Class I, December 1984.

3B-6 McIntyre, T. R. et al., "Mark III Confirmatory Test Program One-Third Scale Pool Swell Impact Tests - Test Series 5805", General Electric Company, NEDE - 13426P, Class III, August 1975.

3B-7 General Electric Company, "Horizontal Vent Confirmatory Test, Part I", NEDC - 31393, Class III, March 1987.

3B-8 Sonin A. A., "Scaling Laws In Small-Scale Modeling of Steam Relief Into Water Pool", ASME Winter Meeting, Chicago, November 1980.

3B-9 Dodge, F. T., "Scaling Study of the GE PSTF Mark III Long Range Program, Task 2.2.1, SwRI", General Electric Company Report NEDE - 25273, March 1980.

3B-10 Mark II Containment Program, "Generic Chugging Load Definition Report", NEDE-24302-P, Class III April 1981.

3B-11 F. J. Moody, "Analytical Model for Estimating Drag Forces on Rigid Submerged Structures Caused by LOCA and Safety Relief Valve Ramshead Air Discharges", NEDE-21471; revised by L. C. Chow and L. E. Lasher, September 1977.

3B-12 L. E. Lasher, “Analytical Model for Estimating Drag Forces on Rigid Submerged Structures Caused by Steam Condensation and Chugging”, NEDO-25153, July 1978.

3B-13 L. E. Lasher, “Analytical Model for Estimating Drag Forces on Rigid Submerged Structures Caused by LOCA and Safety Relief Valve Ramshead Air Discharges”, Supplement for X-Quencher Air Discharge, NEDO - 21471, Supplement 1, October 1979.

3B-14 Not Used.

3B-15 J-H, Chun and A.A. Sonin, “Small-scale Simulation of Vapor Discharge into Subcooled Liquid Pools”, Nuclear Engineering and Design **85**(1985) pp 353-362.

3B-16 Letter, January 20, 1994, General Electric (Jack Fox) to the Staff (Chet Poslusny), “Containment Emergency Procedure Guidelines Issue on Heat Capacity Temperature Limit (HCTL)”, Docket No. 52-001.

3B-17 Toshiba Corporation, "Post LOCA Suppression Pool Swell Analysis for ABWR Containment Design”, UTLR-0005-P, September 2009.

3B-18 Toshiba Corporation, "Condensation Oscillation and Chugging Load", UTLR-0007-P, October 2010.

Table 3B-1 Pool Swell Calculated Values

Description	Value
1. Air bubble pressure (maximum)	195 kPaG
2. Pool swell velocity (maximum)	10.9 m/s
3. Wetwell airspace pressure (maximum)	146 kPaG
4. Pool swell height (maximum)	8.8 m

Table 3B-2 Final ABWR HVT Test Matrix [Proprietary information not included in DCD (Refer to Table 1-1 of the Appendix to UTLR-0007-P)]

Table 3B-3 Not Used

Table 3B-4 Not Used

Table 3B-5 Not Used

Table 3B-6 Not Used

Table 3B-7 Not Used

Table 3B-8 Not Used

Table 3B-9 Not Used

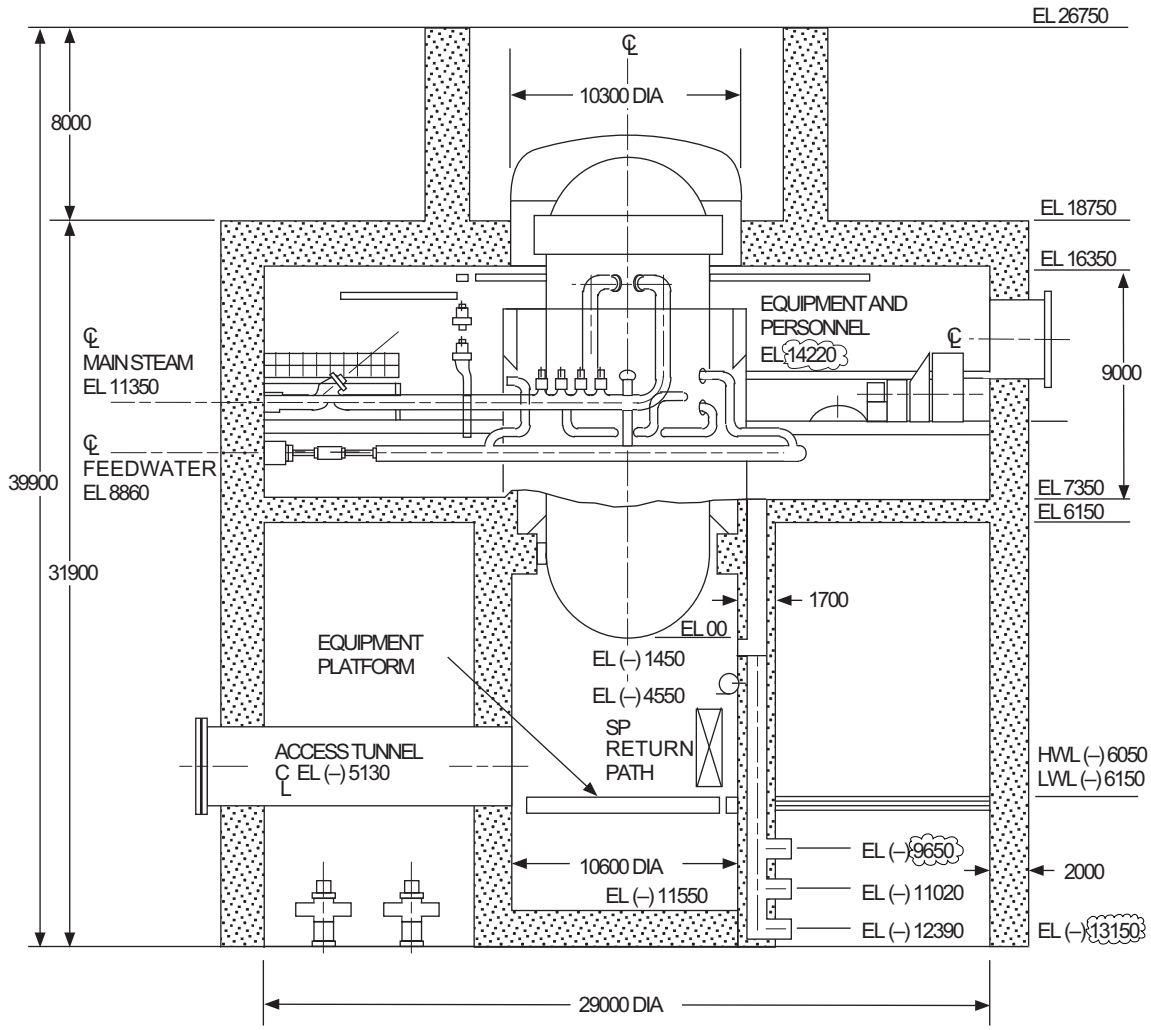

NOTES: DIMENSIONS ARE IN MILLIMETERS
ELEVATIONS ARE WITH RESPECT TO RPV "0"

Figure 3B-1 ABWR Primary Containment Configuration

Figure 3B-2 SRV Quenchers in Suppression Pool [Proprietary information not included in DCD (Refer to Figure 1-2 of UTLR-0007-P)]

Figure 3B-3 Not Used

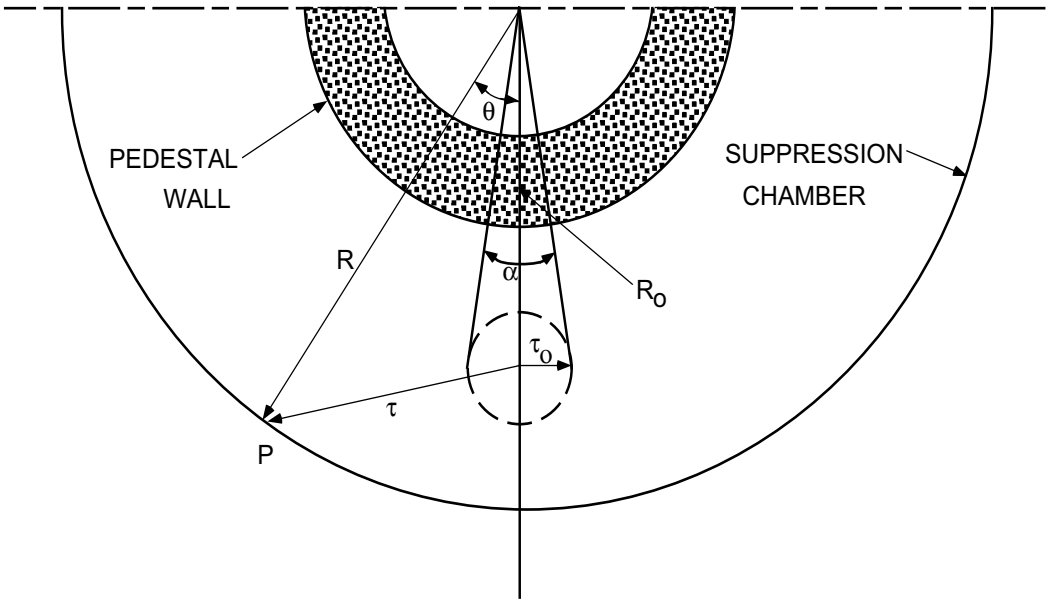

$\tau = R - R_o$: for $\theta < \alpha/2$

$\tau = \sqrt{R^2 + R_o^2 - 2RR_o \cos\theta}$: for $\theta \geq \alpha/2$

Figure 3B-4 Dimensions for P(r) Calculation

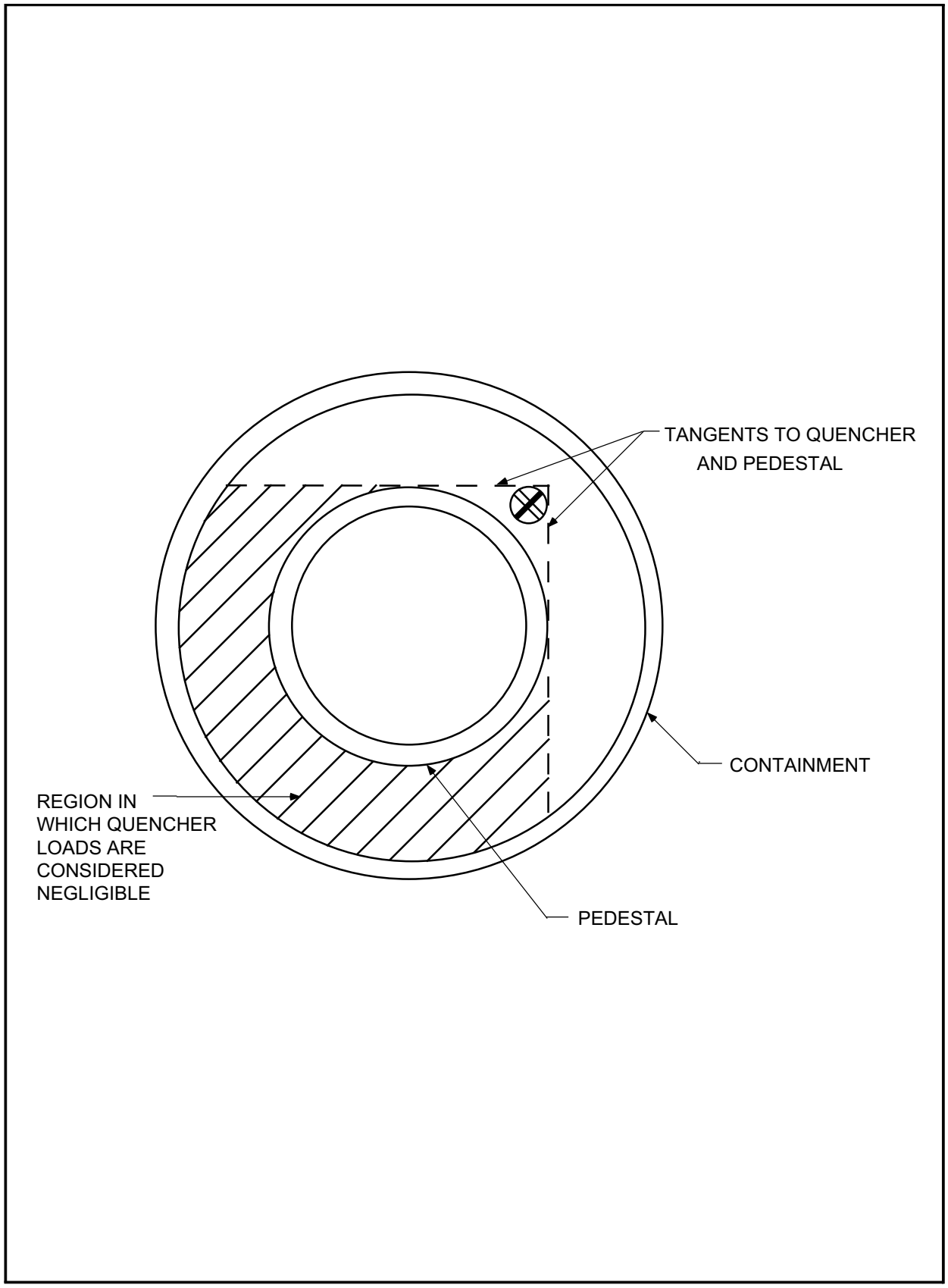

Figure 3B-5 Circumeferential Distribution

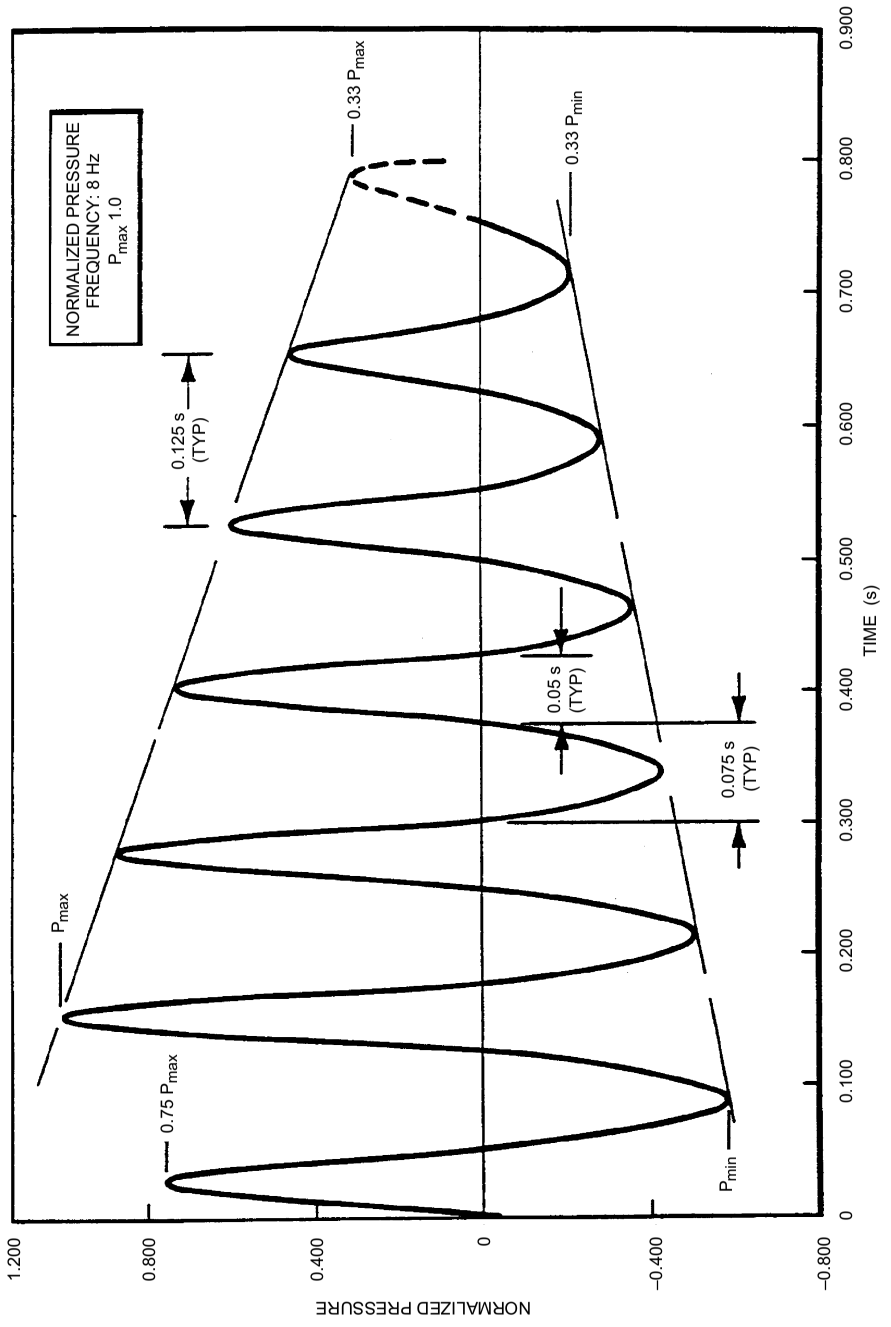

Figure 3B-6 Quencher Bubble Pressure Time History

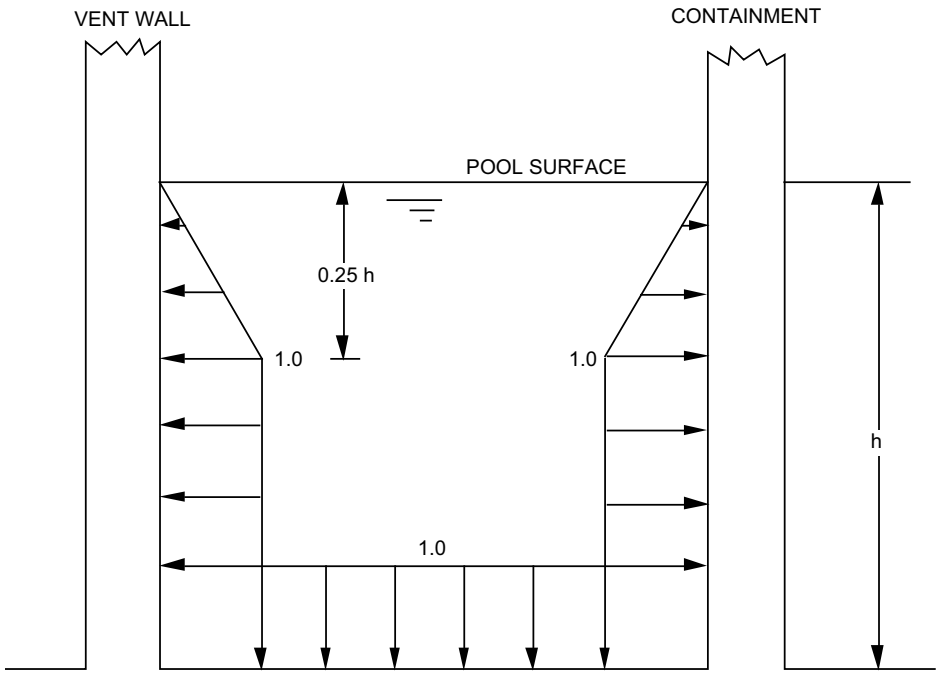

Figure 3B-7 Spatial Load Distribution for SRV Loads

Figure 3B-8 Not Used

Figure 3B-9 Not Used

Figure 3B-10 Not Used

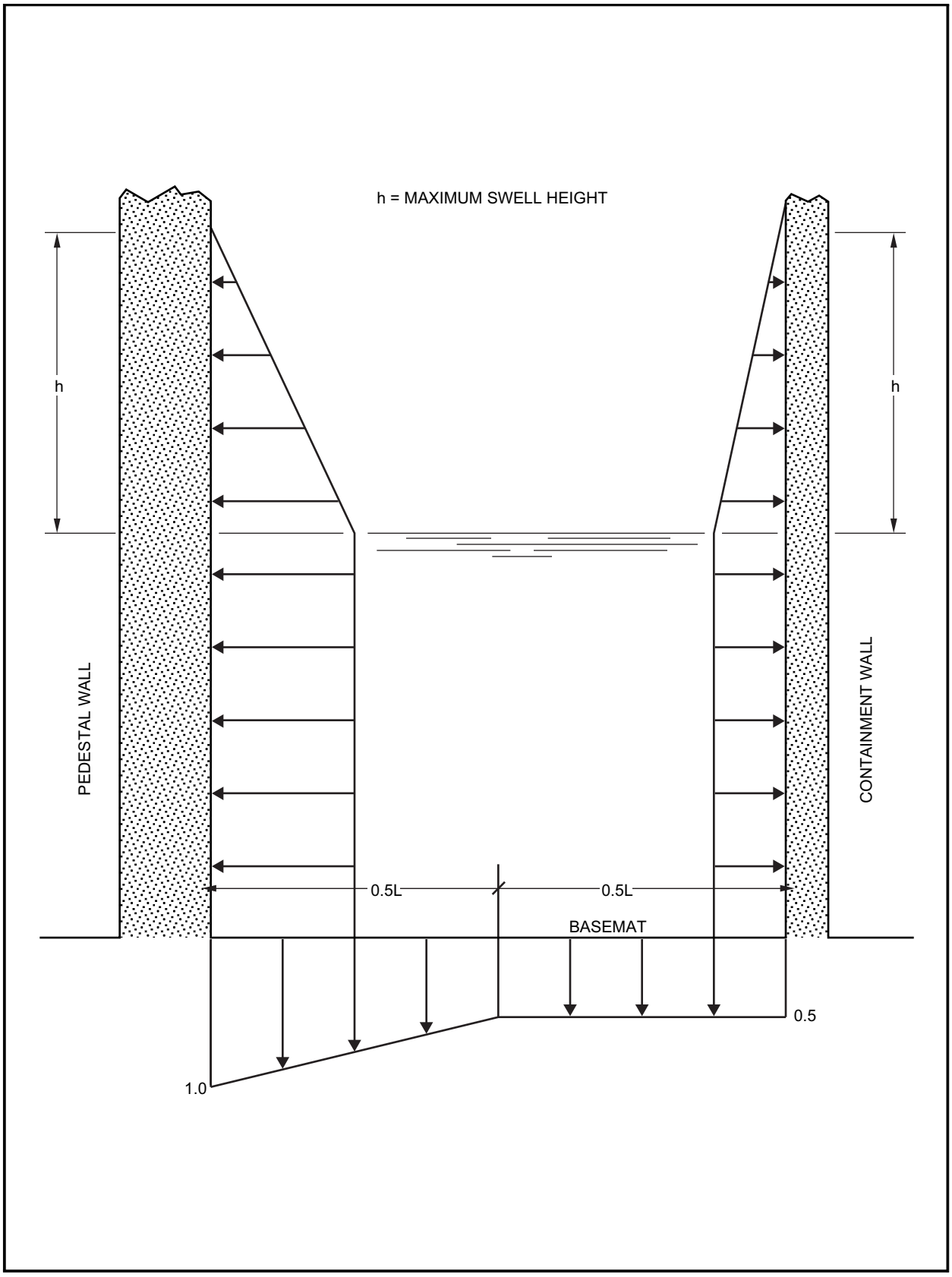

Figure 3B-11 Pool Boundary Pressure During Pool Swell, Normalized to Bubble Pressure

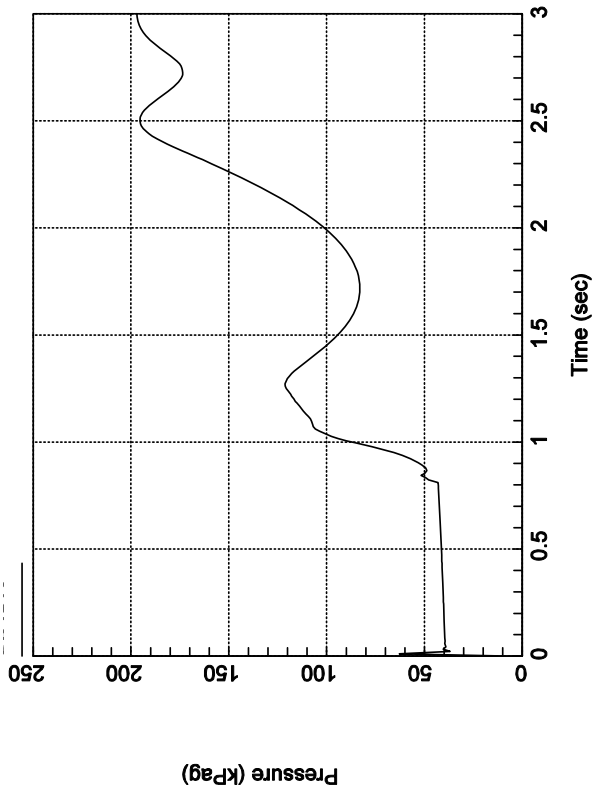

Figure 3B-12 Time History of Air Bubble Pressure

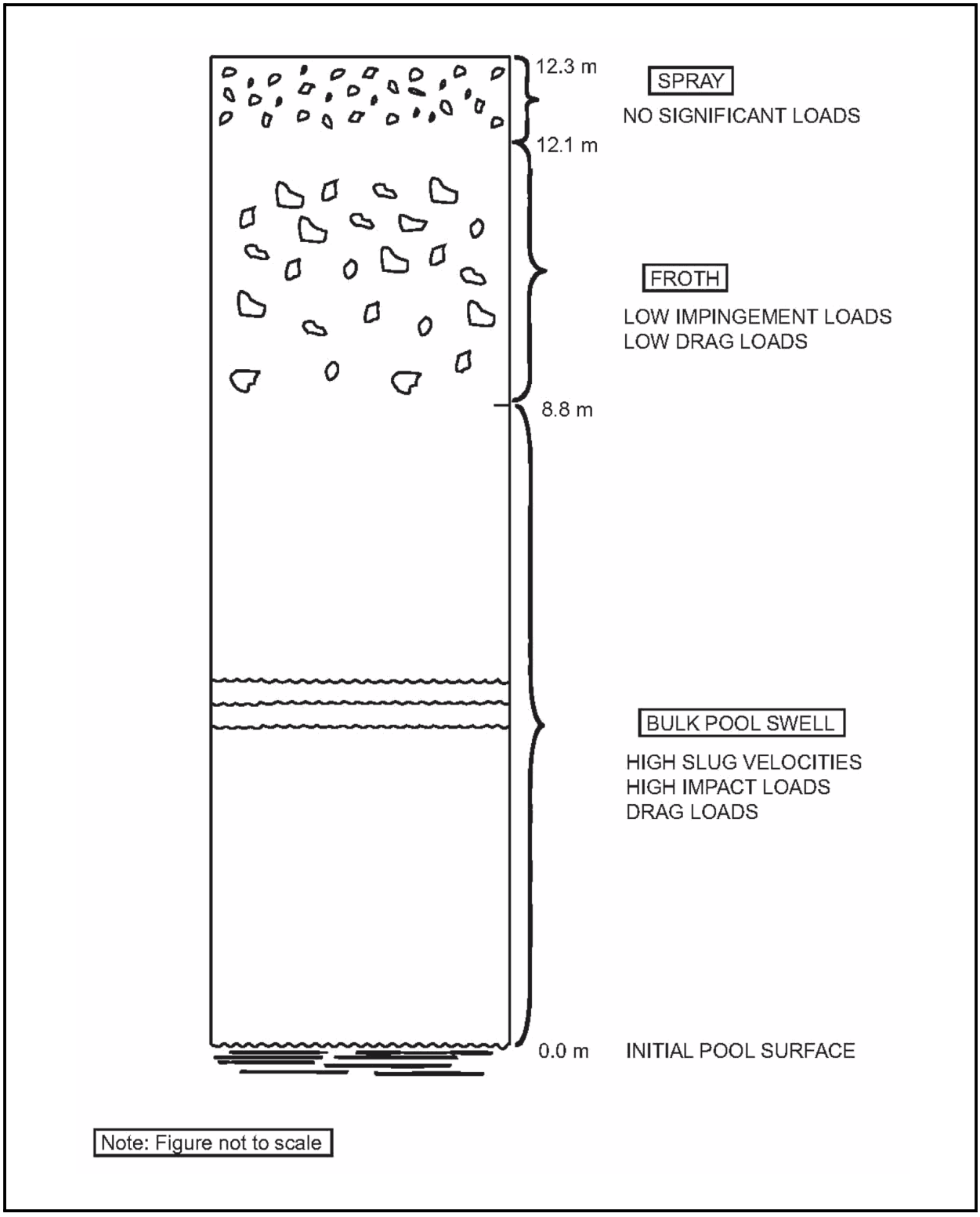

Figure 3B-13 Schematic of the Pool Swell Phenomenon

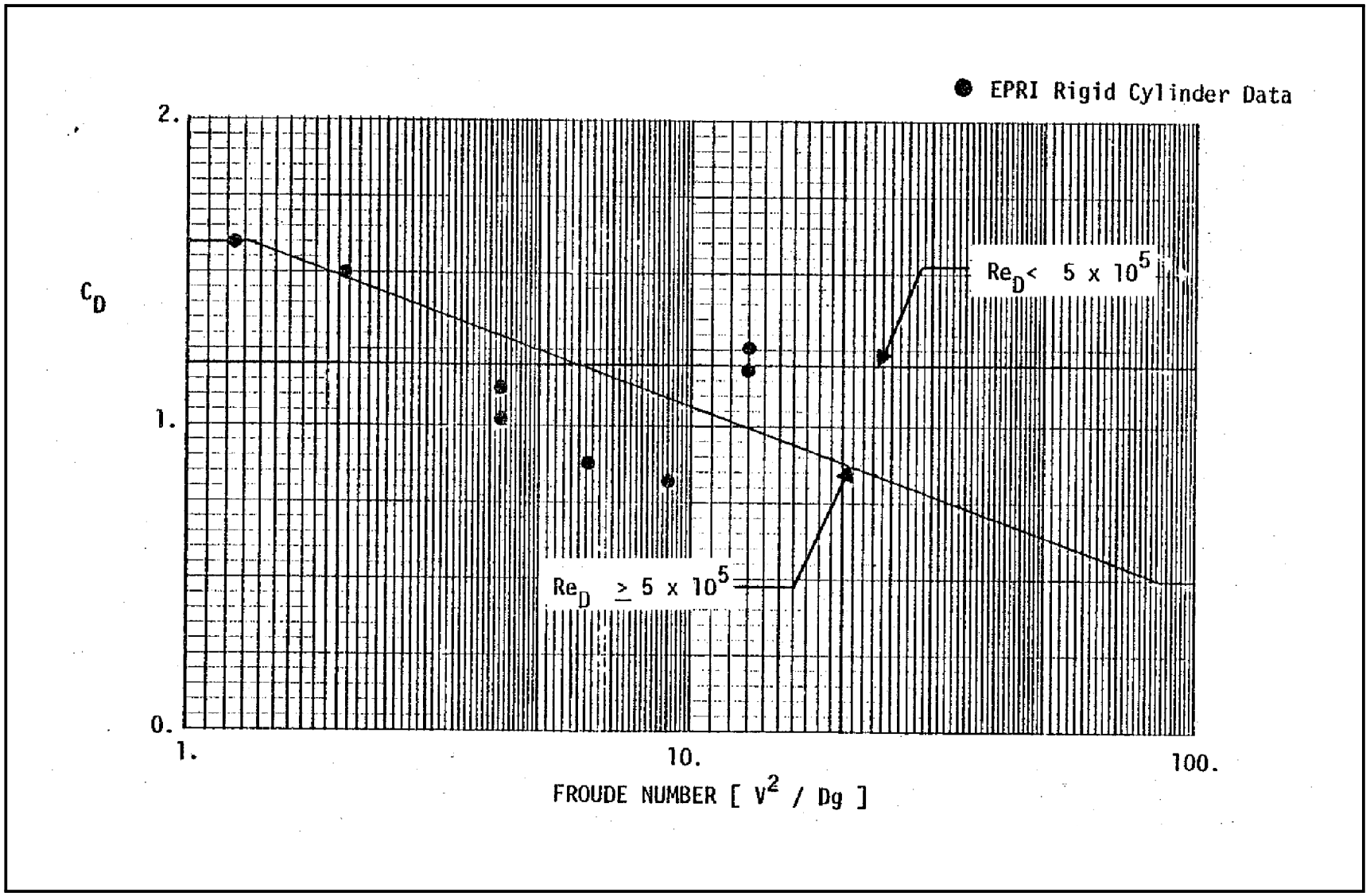

Figure 3B-14 Drag Coefficient for Cylinders Following Impact

Figure 3B-15 Test Facility Outline (1/2.5-Scale) [Information not included in DCD (Refer to Figure 1-1(b) from the Appendix to Toshiba UTLR-0007-NP)]

Figure 3B-16 Test Facility Outline (Full-scale) [Information not included in DCD (Refer to Figure 1-1(a) from the Appendix to UTLR-0007-NP)]

Figure 3B-17 Instrumentation for Drywell and Pressure Suppression Chamber Test [Information not included in DCD (Refer to Figure 1-3 from the Appendix to UTLR-0007-NP)]

Figure 3B-18 Instrumentation of 1/2.5 Scaled Facility (a) and Instrumentation of Actual Scaled Facility (b) [Information not included in DCD (Refer to Figures 1-4 (a) and (b) from the Appendix to UTLR-0007-NP)]

Figure 3B-19 Envelope of the PSD Load of Small-Scaled Test in CO and Analysis (On the 019P Basemat) [Information not included in DCD (Refer to Figure 3.2-2 from UTLR-0007-NP)]

Figure 3B-20 Relationship Between Break Diameter, Pool Water Temperature and CO Oscillation [Information not included in DCD (See Figures 1-6 and 1-7 of the Appendix to UTLR-0007-NP)]

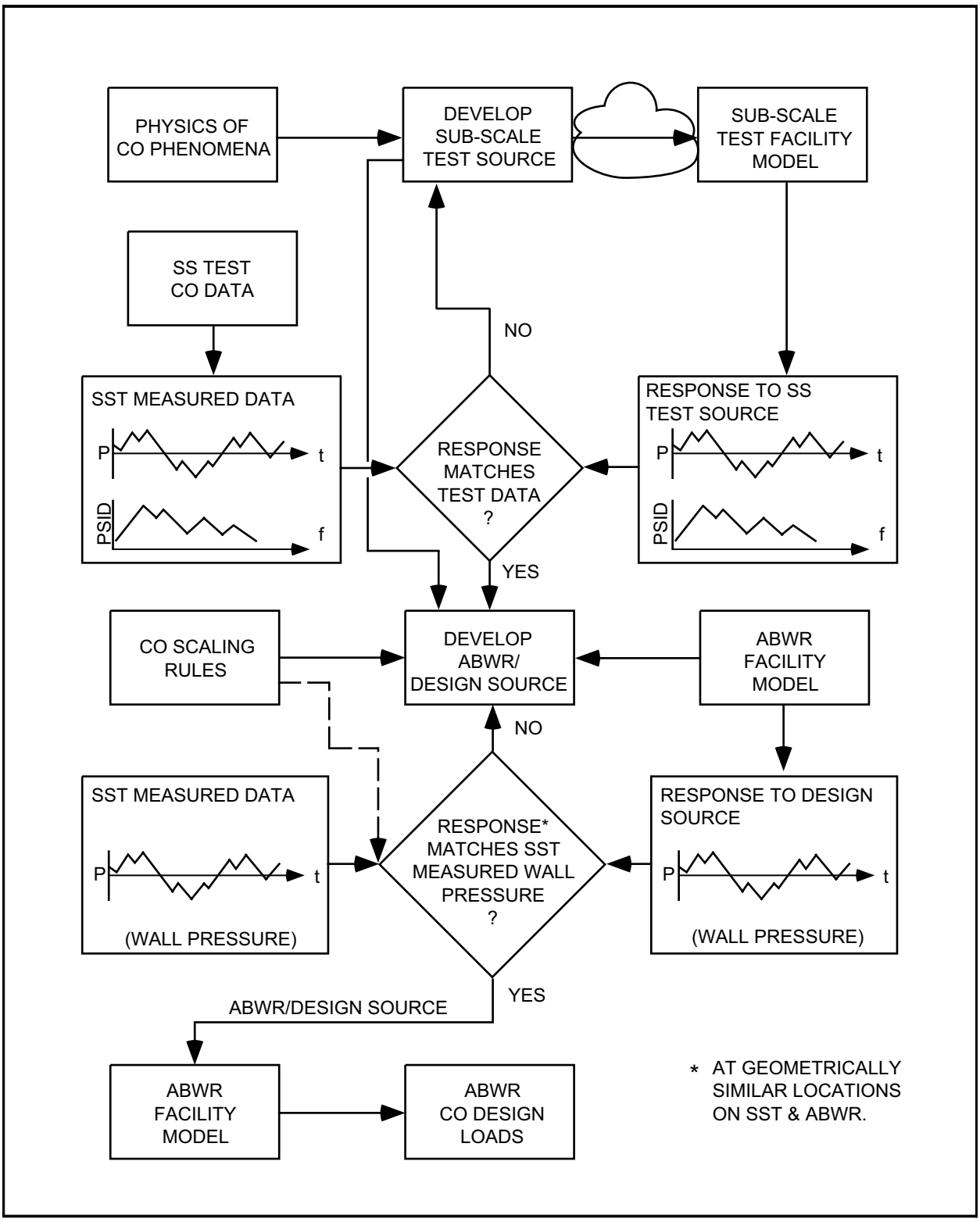

Figure 3B-21 ABWR CO Source Load Methodology

Figure 3B-22 A Typical Pressure-Time History of CO Design Load [Proprietary information not included in DCD (Refer to Figure 3.2-3 from UTLR-0007-P)]

Figure 3B-23 Dependency of Maximum Chugging Occurrence and Pool Water Temperature [Information not included in DCD (Refer to Figure 1-11 from the Appendix to UTLR-0007-NP)]

Figure 3B-24 Typical Chugging [Information not included in DCD (Refer to Figure 1-8(a) from the Appendix to UTLR-0007-NP)]

Figure 3B-25 Chugging PSD [Information not included in DCD (Refer to Figure 1-8(b) from the Appendix to UTLR-0007-NP)]

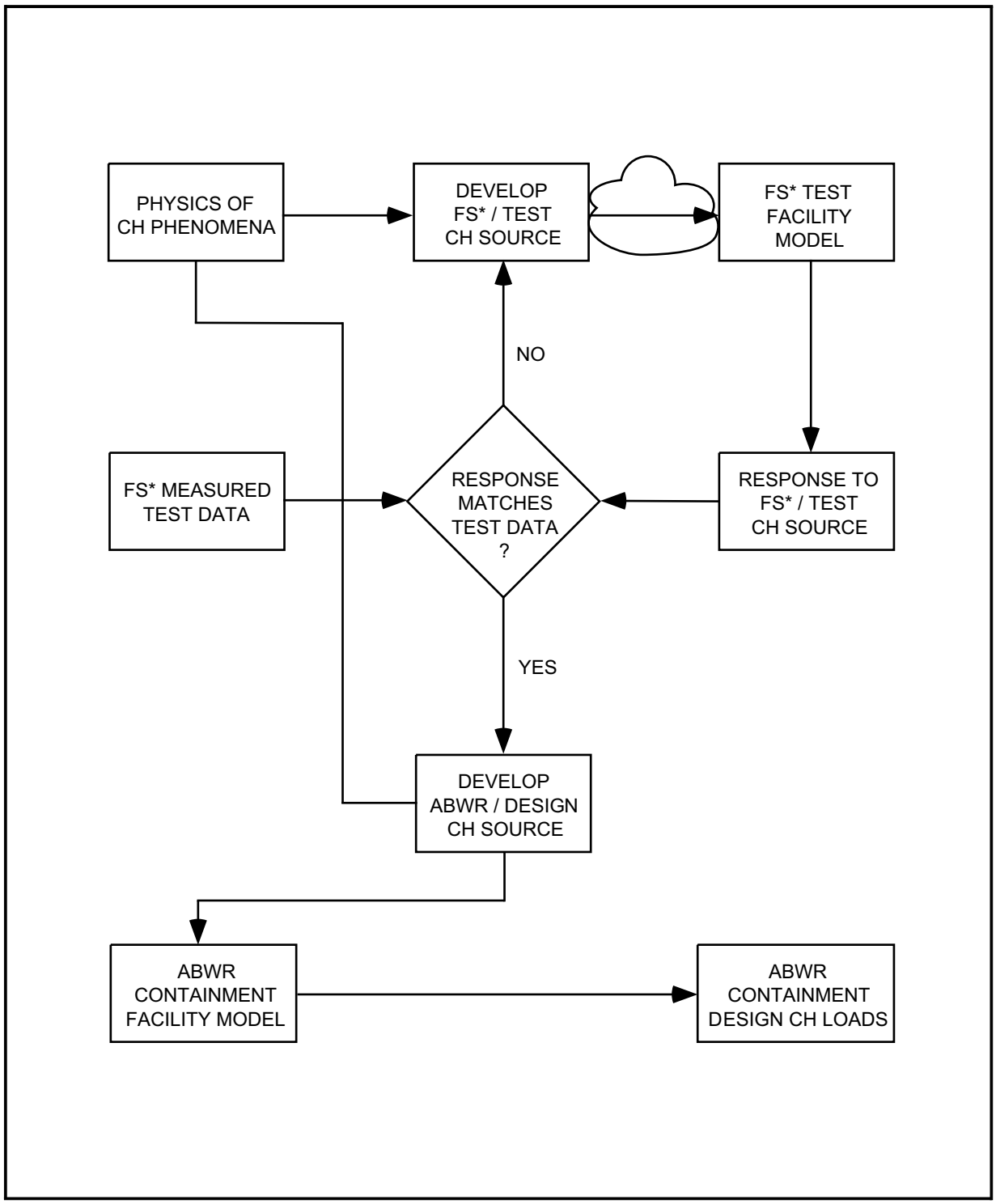

Figure 3B-26 ABWR Chug Source Load Methodology

Figure 3B-27 Comparison of PSD Envelope of Chugging Test Result and PSD Envelope of Design Load [Information not included in DCD (Refer to Figure 3.3-2 from UTLR-0007-NP)]

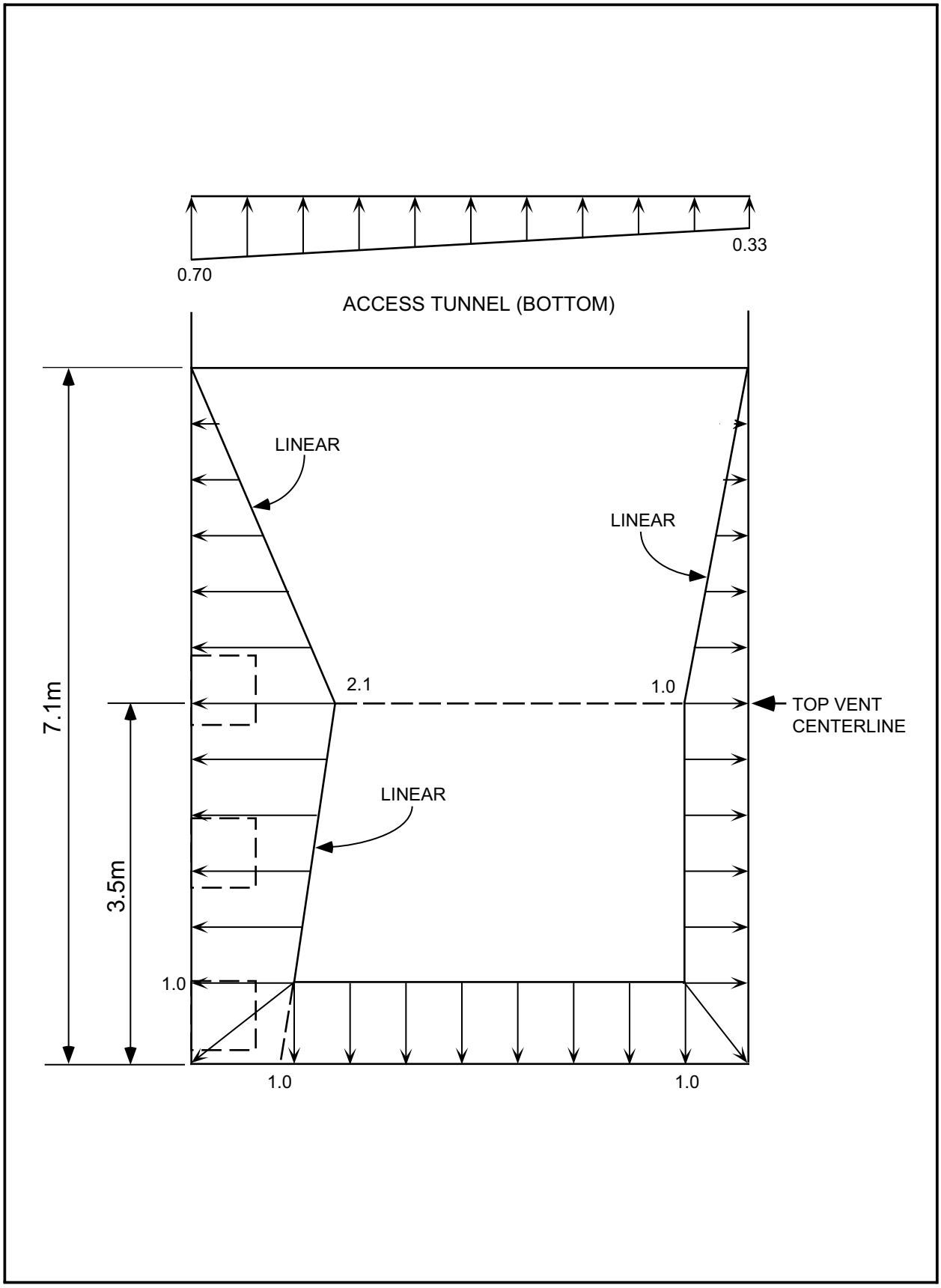

Figure 3B-28 Spatial Load Distribution for CH

Figure 3B-29 A Typical Pressure-Time History of Chugging Design Load [Proprietary information not included in DCD (Refer to Figure 3.3-3 from UTLR-0007-P)]

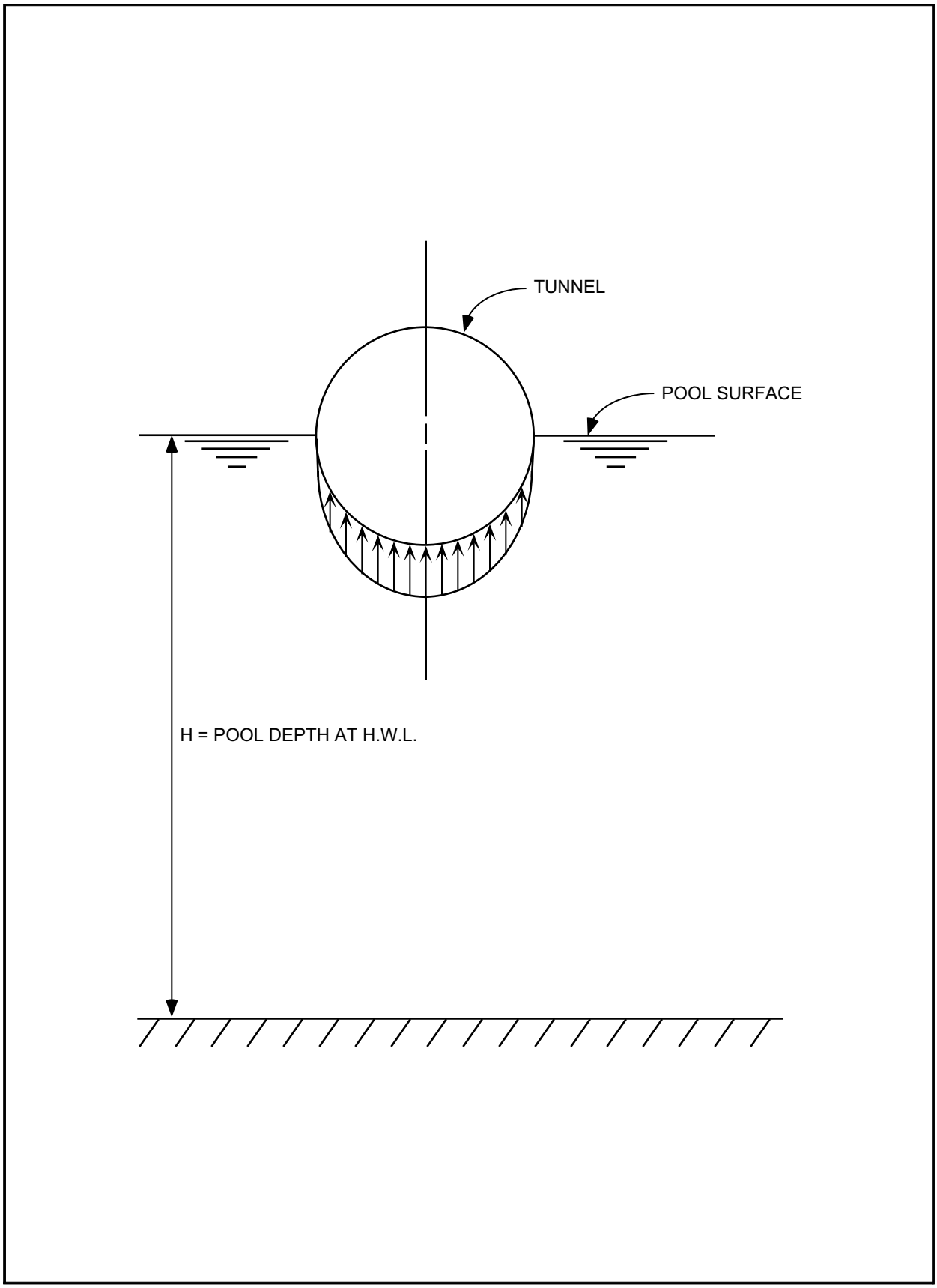

Figure 3B-30 Circumferential Pressure Distribution on Access Tunnel Due to CH

Figure 3B-31 Example of Lateral Load on Horizontal Vent [Information not included in DCD (Refer to Figure 3.3-4 from UTLR-0007-NP)]

Figure 3B-32 Not Used

Figure 3B-33 Design Load of Vent Pipes for Local Chugging [Proprietary information not included in DCD (Refer to Figure 3.3-5(b) from UTLR-0007-P)]

Figure 3B-34 Design Load of Structure Response Analysis for Local Chugging [Proprietary information not included in DCD (Refer to Figure 3.3-5(a) from UTLR-0007-P)]